Floating Foundations in Ice-Infested Waters

Auteur : Nann Shwun Myat Wadi Win,
Promoteur(s) : Rigo, Philippe
Faculté : Faculté des Sciences appliquées
Diplôme : Master : ingénieur civil mécanicien, à finalité spécialisée en "Advanced Ship Design"
Année académique : 2023-2024
URI/URL : http://hdl.handle.net/2268.2/22260

Floating Foundations In Ice-Infested Waters

Supervisor

Matthias Dudek
matthias.dudek@vattenfall.de
Vattenfall Europe Windkraft GmbH

EMship+
Advanced Design

The work in this thesis was carried out in:

VATTENFALL EUROPE WINDKRAFT GmbH.
HAMBURG, GERMANY.

Faculty Supervisor: LIONEL GENTAZ (ECOLE CENTRALE NANTES, FRANCE)

Direct Supervisor: Matthias Dudek (Vattenfall Europe Windkraft GmbH, Germany)

This document was set with LATEXon August 15, 2024.

Declaration of Authorship

I, Nann Shwun Myat Wadi Win, declare that this thesis and the work presented in it are my own and have been generated by me as the result of my own original research.

Where I have consulted the published work of others, this is always clearly attributed.

Where I have quoted from the work of others, the source is always given. With the exception of such quotations, this thesis is entirely my own work.
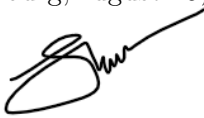
I have acknowledged all main sources of help.

Where the thesis is based on work done by myself jointly with others, I have made clear exactly what was done by others and what I have contributed myself.

This thesis contains no material that has been submitted previously, in whole or in part, for the award of any other academic degree or diploma.

I cede copyright of the thesis in favour of the Ecole Centrale Nantes.

Hamburg,August 15, 2024

_____

Nann Shwun Myat Wadi Win

This page intentionally left blank.

Acknowledgement

I would like to extend my deepest gratitude to my parents, whose unwavering belief in me and steadfast support have been the foundation of all my achievements. Their encouragement has been instrumental in my pursuit of academic and personal aspirations.

I am also profoundly grateful to Professor Philippe Rigo of the University of Liège, who provided me with the opportunity to pursue this master's program. His consistent support and dedication to organizing events aimed at our personal growth and professional networking have greatly enriched my experience.

I would like to express my sincere appreciation to Mr. Matthias Dudek, my supervisor, for his insightful guidance and unwavering support not only during the preparation of this thesis but also throughout my internship at Vattenfall Europe Windkraft GmbH.

My gratitude also extends to Professor Hayo Hendriks of TU Delft for his expert guidance in the specific area of research addressed in this work. His contributions have been invaluable to the development of this thesis.

Additionally, I would like to thank Professor Lionel Gentaz of Ecole Centrale Nantes for his mentorship throughout the entire semester at ECN. His guidance has been critical to my academic progress.

Finally, I am deeply appreciative of my peers, who have stood by me throughout the EMship+ journey. Their support helped me overcome numerous challenges, and their fellowships ensured that I never felt far from home.

This thesis is a testament not only to my own efforts but also to the unwavering support, love, and expertise of these remarkable individuals. I am profoundly grateful to each one of you.

This page intentionally left blank.

Abstract

This thesis examines the challenges and solutions associated with deploying floating offshore wind turbines (FOWTs) in ice-infested waters, focusing on the Baltic Sea region. The primary objective is to develop a comprehensive framework for the design, operation, and maintenance of FOWTs in environments subject to ice loads. Based on the European Green Energy Deal and its goals that are to be achieved by 2050, this study provides important results for sustainable offshore wind farms installed in challenging weather conditions.

To start with, all existing codes and standards designed for both oil and gas exploration and fixed offshore wind turbines are studied in detail. This analysis explores the possibility of applying these codes and standards to floating offshore platforms installed in ice conditions. Parameters considered in this study include ice formation mechanisms, ice thickness, ice mechanical properties, and their interaction with floating platforms. The approach involves numerical modeling and simulations using dynamic simulation software such as Orcaflex to predict the effect of ice loads on tension in mooring lines.

The later part of the study investigates several ice mitigation techniques. The systems generally used include passive mitigation, such as using stronger materials during the structural design stage, and active methods, such as icebreakers and heating techniques. The economic impact of these mitigation techniques is also analyzed concerning both capital expenditure (CAPEX) and operational expenditure (OPEX).

The results highlight the importance of ice management plans and monitoring techniques (for ice mitigation) to reduce the impact of ice loads on floating offshore wind turbines as much as possible. The findings show that as ice loads on the structure increase, there is a greater impact on mooring systems, which directly affects installation expenditures. Operational costs are also affected by higher ice loads.

The findings of this thesis contribute to the body of knowledge on offshore wind energy in cold regions, offering practical solutions and guidelines for the safe and efficient deployment of floating wind turbines in ice-infested waters.

Keywords: Floating Offshore wind turbine, Baltic Sea, Ice Load,Ice Mitigation

This page intentionally left blank.

Table of Content

This page intentionally left blank.

List of Figures

List of Tables

This page intentionally left blank.

List of Abbreviations

Abbreviation	Meaning
BFOW	Bottom Fixed Offshore Wind Farm
BFOWT	Bottom Fixed Offshore Wind Turbines
CAPEX	Capital Expenditure
C$_{\textbf{FDD}}$	Cumulative sum of freezing temperatures
COG	Center of Gravity
DLC	Design Load Case
FDD	Freezing Degree Days
FOWF	Floating Offshore Wind Farm
FOWT	Floating Offshore Wind Turbine
FY	First-year
GW	Gigawatt
IM	Ice Management
MBL	Minimum Breaking Load
MN	Meganewton
NTM	Normal Turbulence Model
O&G	Oil and Gas
OPEX	Operational Expenditure
P1	Point 1
P2	Point 2
P3	Point 3
PSU	Practical Salinity Unit
QTF	Quadratic Transfer Function
RAO	Response Amplitude Operator
SWL	Still Water Line
WTG	Wind Turbine Generator

This page intentionally left blank.

List of Formulas

Symbol	Unit	Meaning
α	deg	Ice cone angle
a	——	Slope of frost index distribution
b	——	Offset of frost index distribution
C_R	MPa	Ice strength coefficient
c	kPa	Apparent keel cohesion
D	m	Width of the ice feature
D	m	Waterline cone diameter in section
D_T	m	Cone top diameter
e	——	Keel porosity
F_D, F_B	MN	Ridge-building action
F_G	MN	Global horizontal crushing ice load
F_R	MN	Horizontal action caused by FY ridge
F_c	MN	Action component due to the consolidated part of the ridge
F_k	MN	Keel action component
f	Hz	Frequency
f_{AR}	——	Empirical term in relation to determine p_G
g	m/s^2	Gravitational acceleration
h, t, t_{open}	m	Ice thickness
h_1	m	Reference ice thickness of 1 meter
h_c	m	Consolidated layer thickness
h_k	m	Vertical distance between the base of the consolidated layer and the base of the keel
h_p	m	Parent ice floe thickness
h_s	m	Sail height
h_{50}	m	Ice thickness in 50-year return period

Symbol	Unit	Meaning
L	m	Clear distance between the legs in section 3.5.8
K, K_{50}	——	Frost index summarized in a winter period
n, m	——	Empirical exponents to take account of the size effect in relation to determine p_G
p_D	MN/m	Ridge-building action per unit width
p_{D0}	MN/m	Ridge-building action per unit width for reference ice thickness h_0
p_G	MPa	External global ice pressure
R	——	Coefficient in relation to determine p_D
T_R	——	Return period
T_a	°C	Mean air temperature (24h) in a frost period
T_f	°C	Freezing temperature of the water
U	m/s	Current speed
V_{hub}	m/s	Mean wind speed at hub height
V_{ice}	m/s	Free ice floe speed
w	m	Width of the structure
γ_w	kg/m^3	Water density
γ_e	——	Effective buoyancy
μ	——	Friction coefficient
μ_ϕ	——	Passive pressure coefficient
ϕ	deg	Angle of internal friction
ρ_i	kg/m^3	Ice density
ρ_w	kg/m^3	Water density
σ_f	Pa	Flexural strength of ice
σ_b	MPa	Bending strength of ice
σ_c	MPa	Characteristic crushing strength of ice

1
Introduction

1.1 Background

The transition to renewable energy sources has become a global priority, driven by the urgent need to mitigate climate change and enhance energy security. Wind energy, in particular, has emerged as a cornerstone of this transition, offering a suitable and scalable solution to meet rising energy demand. According to the Global Wind Energy Council's (GWEC) 2023 report [1], nearly 78 GW of wind power capacity was added worldwide in 2022, bringing the total installed capacity to 906 GW, reflecting a year-on-year growth of 9% [1]. This growth is expected to accelerate, with projections driven by significant policy initiatives and investments across major economies such as the United States, China, and the European Union [1].

(a) New wind power capacity in 2022 by region (%)[1]

(b) New Installation [1]
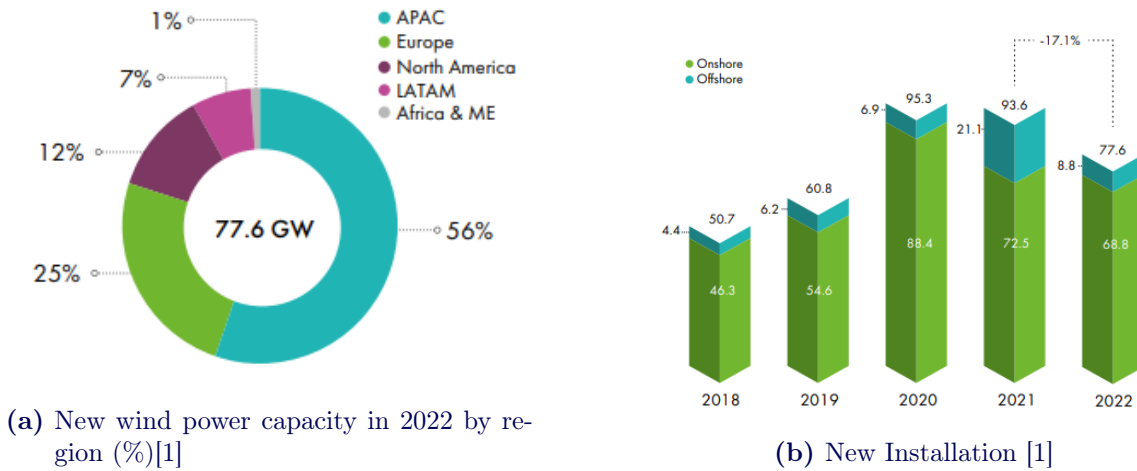
Figure 1.1: Wind power capacity

In Europe, wind energy plays a critical role in meeting the continent's ambitious renewable energy targets. The EU Green Deal has set the goal of making the entire European Union climate neutral by the end of 2050. All fossil fuels are to be replaced by renewable sources as stipulated in the REPowerEU program, which will also ensure energy security. As of 2023, 18.5 GW of wind power capacity has been added to the European grid, of which 16.2 GW is supplied by the EU, demonstrating a firm commitment to the Green Deal.

Germany is leading in this regard with 69.5 GW of renewable electricity capacity. Recently, 3.2 GW of electricity generated from renewable sources was added. Similarly, the Netherlands added 2.8 GW to their grid using renewable sources, bringing their total renewable capacity to 11 GW. Additionally, France added 2.6 GW, making the total capacity 23.5 GW. Sweden added 2 GW, making the total capacity 16.3 GW. The United Kingdom recently added 1.4 GW, bringing the total capacity to 30.2 GW. Poland added 1.4 GW, making the total capacity 9.4 GW. Finland added 1.3 GW, making the total capacity 6.9 GW [2]. Medium-sized markets

such as Greece, Italy, Austria, Belgium, and Croatia also made substantial contributions to the European wind energy sector according to the WWEA report [2].

The primary driver behind Europe's push towards renewable energy, apart from addressing climate change, is the goal of reducing dependence on imported fossil fuels. The European Commission and most EU member states have thus prioritized renewable energy, placing it at the forefront of their energy agendas.
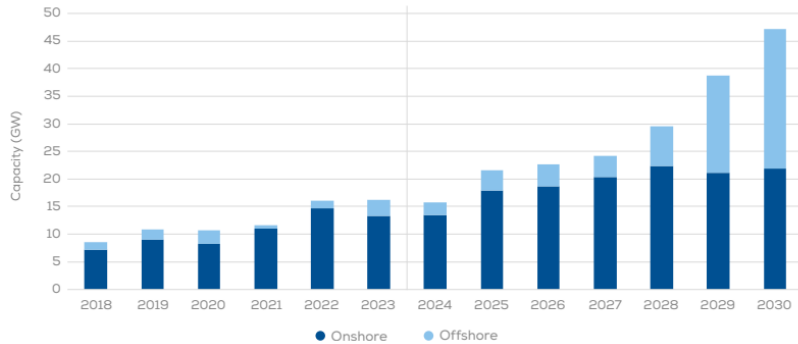
Figure 1.2: 2024-30 annual onshore and offshore wind power installations in the EU - WindEurope's Outlook.[3]

1.2 Problem Statement

The deployment of floating offshore wind farms (FOWF) in the Baltic Sea region represents a promising approach to achieving Europe's renewable energy targets and reducing reliance on fossil fuels. However, these installations face significant challenges due to the unique conditions of ice-infested waters in the Baltic Sea. The Baltic region experiences ice generation phenomena, which involve level ice, ridges, and floes. Consequently, the floating platforms will experience loads generated by this ice, which in turn will affect the mooring lines and could compromise the integrity of the structure. This makes it necessary to have a detailed design and ice mitigation strategies. Due to wind conditions and ice cover across the Baltic Sea, these factors pose a challenge for floating offshore wind farms.

In this regard, the already established research and knowledge employed in the oil and gas industry as well as in the bottom-fixed offshore wind farms operating in ice-prone regions provide a good starting point to develop the methodology which can be used to model the interaction between ice and floating offshore wind farms. Floating systems have different operational methods, and the dynamics of floating structures are also different compared to bottom-fixed systems. Therefore, the straightforward and direct application of methods devised for fixed structures to floating structures is not effective enough and can be expensive as well.

Thus, the main goal is to investigate the feasibility of cost-effective strategies to deploy floating structures operating in icy waters. In this study, this has to be done for the Baltic region. Site-specific ice data is needed for the estimation of ice loads according to the selected region, e.g., ice thickness, ice speed, and air temperature, etc. Evaluating the detailed ice conditions is essential to determine how well IM system can be applied to this region.

1.3 Project Objectives

The importance of floating offshore wind farms is undeniable, particularly in highlighting the increased potential of areas that cannot be covered with bottom-fixed offshore (BFOW) technology. Due to this, they are crucial for the EU to achieve its Green Energy Deal goals. For this purpose, detailed research is needed. The aims of this thesis are listed below:

1. **Analyze Existing Standards:** Review and adapt existing codes and standards from the O&G and BFOW sectors to address the specific needs of FOWF in ice-infested waters. This involves evaluating the adaptability of these standards to ensure cost-efficient applicability and highlighting the differences in requirements.

2. **Evaluation of Ice Management Strategies:** Feasibility assessment of existing ice management plans and ice mitigation strategies. Identification of different ways in which ice is formed, and their effects on floating offshore wind farms. The evaluation of appropriate ice mitigation strategies is also needed.

3. **Design for Ice Loads:** Develop methodologies to estimate ice loads due to different ice formations on floating structures. This involves deducing the consequences for mooring design by comparing ice loads with ULS loads, and highlighting other affected subsystems and their necessary adaptations.

4. **Cost Assessment:** Evaluate differences in CAPEX and OPEX estimates due to changes in mooring lines and the incorporation of ice mitigation strategies as one of the objectives of this study.

The outcome of this research will provide a comprehensive framework for designing and operating floating offshore wind farms in ice-prone areas. This will ensure their safety, reliability, and economic viability while contributing to the achievement of climate-neutral goals.

This page intentionally left blank.

2

State of the Art

As far as operations in icy waters such as the Arctic are concerned, oil and gas platforms have been operating in these conditions for a significant period of time. Due to this, standard design procedures and guidelines have already been established. For Arctic offshore structures, ISO 19906 provides specific guidelines related to design, construction, and operation, ensuring that no issues related to safety and reliability occur. Mostly, these procedures are for load estimation due to ice formation, and selection of appropriate materials that should sustain the extreme climate [7]. One example of such a platform is the Molikpaq platform in the Beaufort Sea, which can sustain ice loads of up to 5 MN [25].

Bottom-fixed offshore wind turbines (BFOWTs) are commonly used in shallow to medium-depth waters where their foundations are anchored directly to the seabed. These structures, typically monopiles or jackets, are designed to withstand environmental loads from wind, waves, and currents. In ice-prone areas, BFOWTs must also handle ice loading. Conical structures at the waterline are often used to convert horizontal ice forces into vertical forces, promoting the bending failure of the ice sheet and reducing the impact on the turbine [8]. Europe has seen significant BFOWT deployments, particularly in the North Sea and the Baltic Sea. In 2023, Europe added 2.9 GW of new offshore wind capacity, bringing the total to 30 GW, with significant contributions from the UK, Germany, and the Netherlands [1].

For the installation of wind farms in deeper waters, where wind characteristics are favorable, bottom-fixed offshore structures cannot be built economically because of excessive water depth. In these areas, floating structures come into play, which are generally moored. Extensive research on ice and structure interaction is needed because FOWTs in icy waters are a relatively new concept, and standards are still in development [26]. Until 2023, the total installed electricity capacity generated using FOWTs reached 200 MW. A couple of examples are the Hywind Scotland wind farm, which has a capacity of 30 MW, WindFloat Atlantic with a capacity of 25 MW, and the latest FOWF, Hywind Tampen, with 88 MW [1].

The Baltic Sea experiences seasonal ice coverage, presenting unique challenges for offshore wind turbines. Ice loads on structures depend on ice thickness, drift speed, and the mechanical properties of the ice. Ice interactions with offshore structures can lead to crushing and bending failures, depending on the structure's geometry and the ice's properties [27]. The Baltic Sea's ice conditions are generally lighter than those of the Arctic, with typical design ice thicknesses ranging from 0.3 to 1.2 meters. However, the variability and unpredictability of ice conditions, combined with the impacts of climate change, necessitate specialized design and operational strategies to ensure the safety and efficiency of offshore wind turbines in this region [29].

The study by Høyland involves the development and validation of ice mitigation techniques due to loads induced on structures by ice. Based on technology developed for oil and gas

platforms, this study is essentially an effort to increase existing knowledge regarding FOWTs and their interaction with ice. The region for this study is the Baltic region. Furthermore, the development of numerical techniques and dynamic simulations to mimic the behavior of structures in response to ice is also studied. Additionally, effective ice mitigation strategies, including ice cones to decrease the effect of ice-structure interaction, are studied. This study is conducted to create proper guidelines specific to floating systems operating in icy conditions in the Baltic region [27, 29].

Deploying FOWTs in ice-infested waters presents both challenges and opportunities. The dynamic nature of floating structures allows them to move with waves, wind, and more importantly with the ice, potentially reducing the impact of ice loads. However, the interaction between floating structures and ice is complex and not yet fully understood. The main challenges in this study are the effects of ice loads on the FOWT foundation and substructures. The effect of mooring lines on load distribution and stress profiles on the floater is also very critical because ice loads can damage the mooring lines as well [25]. Mooring lines can fail due to ice loads on the floater itself. Moreover, the environmental footprint of FOWTs also needs to be considered. The aquatic ecosystem is affected by FOWT operations, and its consideration is necessary. Therefore, a good balance between the environmental effects of FOWTs and the methods to reduce the environmental footprint as much as possible is needed [27].

Although extensive research is being done in the BFOW sector, there is still a knowledge gap when it comes to the determination and mitigation of ice loads on floating offshore wind turbine platforms. One reason behind this is the unavailability of data in the Baltic region related to ice-structure interaction and ice conditions. This makes it inevitable to gather as much data as possible for this region. Such platforms would be crucial for validating and refining numerical models. Although the Nordströmsgrund platform has provided valuable data, more extensive and contemporary datasets are needed to address current challenges [29].

Moreover, the development of standardized methods for determining ice design parameters and assessing structural responses to ice loads is essential. This includes creating guidelines for floating structures in ice-prone waters, which are currently underdeveloped. Existing standards, such as ISO 19906, require adaptation to address the specific conditions of the Baltic Sea and floating wind technologies [7, 8]. Another critical area for future research is understanding the impacts of climate change on ice conditions in the Baltic Sea and incorporating these insights into design and operational strategies. Climate models predict changes in ice cover and thickness, which will significantly affect load predictions and design criteria [29].

Finally, continued research and development of innovative design solutions, such as semi-active control systems and adaptive structural components, are needed to enhance the resilience of offshore wind turbines to ice loads.

3
Methodology

The entire workflow of the thesis is shown in Figure 1.2, and the process begins with the analysis of engineering standards related to ice conditions. Following this, the types of ice present in the area are assessed in specific design locations in the Baltic Sea. Ice load evaluations on floaters are conducted to understand the impact of ice on these structures. Next, Design Load Cases (DLC) are defined, and simulations of these load cases are performed using the OrcaFlex software. The simulation results are used to assess the effective tension in the mooring lines. A critical check is conducted to ensure that the effective tension does not exceed 60% of the mooring line's Minimum Breaking Load (MBL) [16]. If the tension exceeds this limit, new mooring lines are selected, and the additional cost due to these upgraded lines is estimated. If the tension remains within acceptable limits, cost-effective ice mitigation strategies to reduce ice loads are proposed. The process concludes after these steps are completed, as illustrated in figure 3.1.
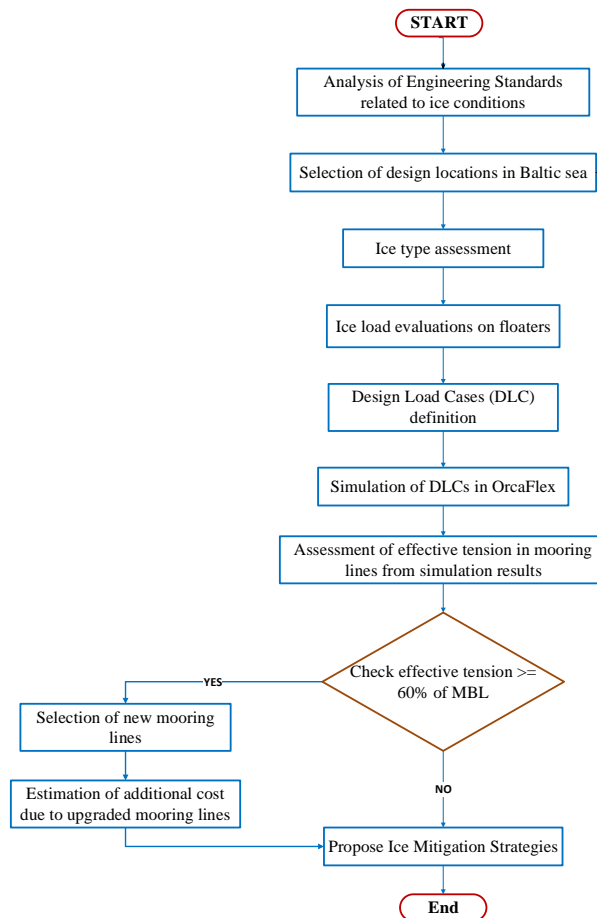
Figure 3.1: FlowChart

3.1 Codes and Standards for the Ice-infested Area

In the development and assessment of offshore wind turbines, particularly in ice-prone areas, the application of internationally recognized standards and codes is of the utmost priority in the design stage. These standards ensure the structural integrity, safety, and reliability of the installations. Below is a discussion of the key standards used in this study and their significance:

1. **IEC 61400-3-1:2019 - Wind Turbines - Part 3-1:** Design Requirements for Offshore Wind Turbines [13]

2. **IEC 61400-3-2:2019** - Design Requirements for Floating Offshore Wind Turbines [14]

3. **ISO 19906:2019** - Petroleum and Natural Gas Industries - Arctic Offshore Structures [7]

4. **DNV-ST-0437:2016** - Loads and Site Conditions for Offshore Wind Turbines [8]

5. **DNV-OS-J101:2014** - Design of Offshore Wind Turbine Structures [11]

6. **DNV-OS-J103:2013** - Design of Floating Wind Turbine Structures [10]

7. **ABS Guide for Building and Classing Floating Offshore Wind Turbine Installations** [15]

The application of these standards is crucial in various aspects, especially in the ice-prone environment. They not only serve as guidelines but also provide safety in all design stages. Most importantly, they ensure the structural integrity, recommend ice mitigation systems, provide empirical formulations from the collected field data, identify the risk and suggest safety factors in different design configurations, such as environmental loads, dynamic loads, etc. Furthermore, adhering to these standards can yield better design optimization, resulting in cost-effective designs.

3.2 Climate Properties in Baltics Sea

3.2.1 Air Properties, Temperature, and Salinity

At different depths, salinity sensing probes are installed at FINO2 measurement station. Salinity at an average depth of 2m is 8.5 PSU during winters. At this value of salinity, water freezes at around -0.45°C [13]. Salinity is important to be ascertained as the density of water and ice formation are affected by it.

Seawater density varies with salinity and temperature. According to [13], the density of seawater ranges between 1003 and 1014 kg/m³. A typical density for seawater is around 1007 kg/m³ in the Baltic region [12]. This density is influenced by the amount of dissolved salts (salinity) and the temperature of the water. As water cools and approaches its freezing point, its density increases until it reaches the maximum density at around 4°C, after which it decreases as it freezes.

The density of sea ice is an important factor in the context of floating offshore wind turbines. The density of sea ice depends on its salinity, temperature, and age. Freshly formed sea ice tends to have higher salinity and density, but as it ages, brine pockets within the ice drain

out, reducing its salinity and hence its density. Typical values for sea ice density range from 912 to 925 kg/m³ [12]. For the west Baltic Sea, an average value of 920 kg/m³ is often used [12].

This variation in density affects the buoyancy and stability of floating structures. Higher density seawater provides greater buoyant force, which is beneficial for floating wind turbines. On the other hand, the difference in water density and ice formation mechanisms induces additional forces on floating offshore structures. The interaction between ice and structure will of course affect the structures.

3.2.2 Metocean Data from DHI

If ice loads on the offshore structure are to be estimated, wind, wave, and current data are required and for this study, this data was collected from the DHI website. This data consists of wind speed, its direction, wave height, and wave peak periods, current speed over a specific period of time , and this gives complete information about the environmental conditions in the region.

Different data visualizations and statistics were gathered from the metocean data. Data is in the form of scatter plots, extreme condition distributions, monthly statistics, frequency distributions, and rose plots. This provides a good comparison between model data and data gathered from satellites. These visualizations collectively help understand the variability, trends, and extreme conditions of these environmental parameters, which are critical factors influencing ice formation and movement.

Key insights from the data include the following: The scatter plots and associated metrics, such as the correlation coefficient and mean absolute error, validate the accuracy of the data from different sources for wind, wave, and current measurements. Extreme condition analysis using the Gumbel distribution estimates the return periods and intensity of severe wind, wave, and current events, which are critical for assessing maximum ice loads. To ascertain the seasonal variation in metocean data like wind speeds, wave data, and current data, monthly statistics are used. Observing the monthly statistics reveals that during winters, values of these environmental parameters increase , which ultimately affects ice formation and growth. If the frequency of these parameters needs to be determined, frequency distribution plots are a good way to check. Rose plots mostly tell about the directions from which these parameters generally originate.

These data-driven insights guide the next steps in ice load estimation by incorporating wind, wave, and current effects into the calculation of ice thickness. This involves using these environmental parameters to model ice dynamics, including formation, growth, and movement. The extreme values inform the upper bounds of ice loads, ensuring that the design of offshore structures accounts for the worst-case scenarios. Seasonal trends help in understanding the periods of maximum risk, enabling proactive planning and mitigation strategies.

The detailed analysis of wind, wave, and current data from the DHI website provides a solid foundation for accurately estimating ice thickness and, consequently, ice loads. These estimates are crucial for designing offshore wind turbines and other structures to withstand

the challenging conditions in ice-prone areas. The integration of this data into ice load models ensures robust, safe, and reliable designs, meeting the stringent requirements of standards and codes. The data for Point 1 is presented below as an example, with additional visualizations and detailed analyses available in the appendix A.1 for both Point 2 and 3 as well.

Wind Data

Here wind data is presented and definition of quality indices are listed down.

Definition of Quality Indices

$$\overline{Y} = \frac{1}{N} \sum_{i=1}^{N} Y_i \tag{3.1}$$

$$\overline{X} = \frac{1}{N} \sum_{i=1}^{N} X_i \tag{3.2}$$

$$STD_Y = \sqrt{\frac{1}{N-1} \sum_{i=1}^{N} (Y - \overline{Y})^2} \tag{3.3}$$

$$STD_X = \sqrt{\frac{1}{N-1} \sum_{i=1}^{N} (X - \overline{X})^2} \tag{3.4}$$

$$Bias = \frac{1}{N} \sum_{i=1}^{N} (Y - X)_i = \overline{Y} - \overline{X} \tag{3.5}$$

$$AME = \frac{1}{N} \sum_{i=1}^{N} |(Y - X)_i| \tag{3.6}$$

$$RMSE = \sqrt{\frac{1}{N} \sum_{i=1}^{N} (Y - X)_i^2} \tag{3.7}$$

$$SI = \frac{\sqrt{\frac{1}{N} \sum_{i=1}^{N} (Y - X - \text{BIAS})_i^2}}{\frac{1}{N} \sum_{i=1}^{N} |X_i|} \tag{3.8}$$

$$EV = \frac{\sum_{i=1}^{N} (X_i - \overline{X})^2 - \sum_{i=1}^{N} [(X_i - \overline{X}) - (Y_i - \overline{Y})]^2}{\sum_{i=1}^{N} (X_i - \overline{X})^2} \tag{3.9}$$

$$CC \; = \; \frac{\sum_{i=1}^{N}(X_i - \overline{X})(Y_i - \overline{Y})}{\sqrt{\sum_{i=1}^{N}(X_i - \overline{X})^2 \sum_{i=1}^{N}(Y_i - \overline{Y})^2}} \tag{3.10}$$

$$QQ \; = \; Linear \;\; least \;\; square \;\; fit \;\; to \;\; quantiles \tag{3.11}$$

$$PR \; = \; \frac{\sum_{i=1}^{N_{\text{peak}}} y_i}{\sum_{i=1}^{N_{\text{peak}}} x_i} \tag{3.12}$$

where

N: Number of data points (synchronized)

$\overline{Y}$: Mean of Y data

$\overline{X}$: Mean of X data

STD_Y: Standard deviation of Y data

STD_X: Standard deviation of X data

Bias: Mean Difference

AME: Absolute Mean Difference

RMSE: Root Mean Square Difference

SI: Scatter Index (unbiased)

EV: Explained Variance

CC: Correlation Coefficent

QQ: Quantile- Quantile (Linear least square fit to quantiles)

PR: Peak ratio
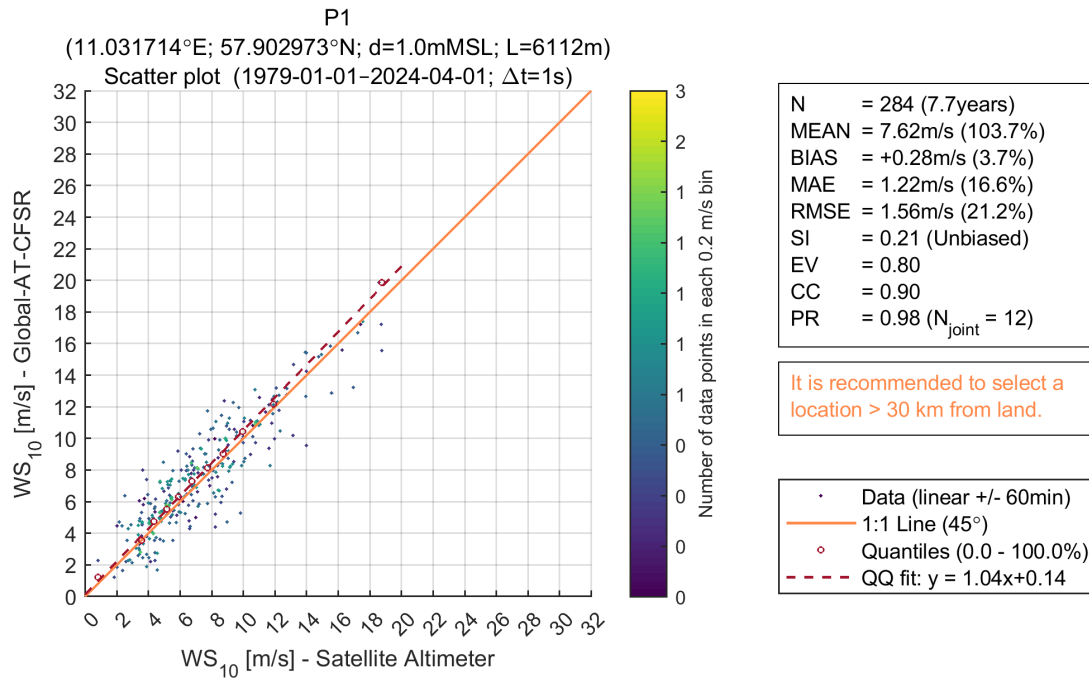
Figure 3.2: Wind Speed Satellite Altimeter Data of Point 1 from DHI

Wave Data
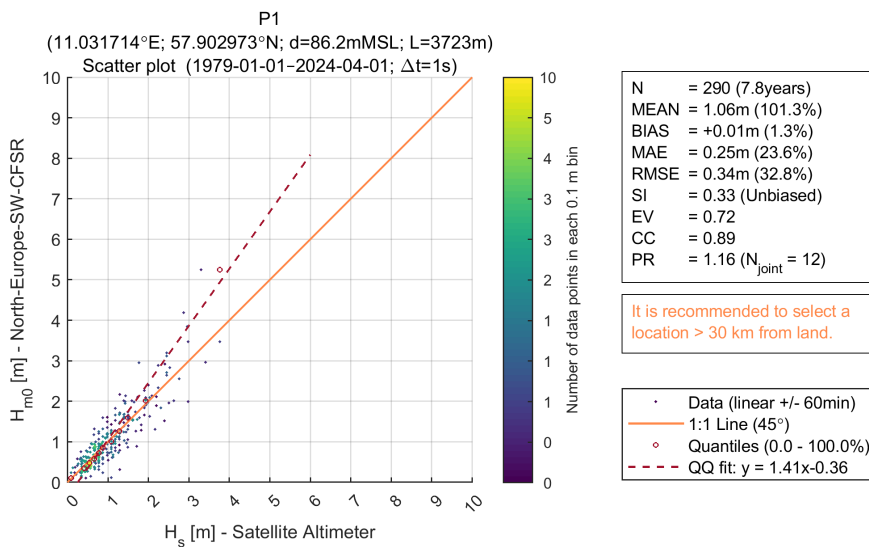
Figure 3.3: Wave Satellite Altimeter Data of Point 1 from DHI

Current Data
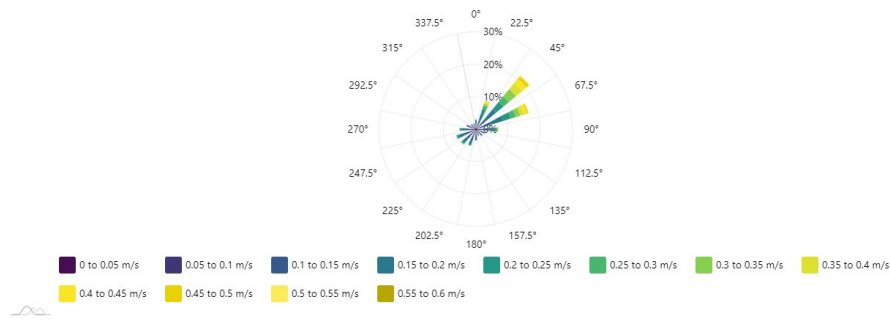
Figure 3.4: Current Data of Point 1 from DHI

3.3 Design Points in the Baltic Sea

The Baltic Sea, a marginal sea of the Atlantic Ocean, is enclosed by several countries including Sweden, Denmark, Finland, Estonia, Latvia, Lithuania, Poland, Germany, and Russia. It is characterized by unique oceanographic and climatic conditions that pose challenges for offshore wind energy projects, particularly due to the presence of ice during winter months. The following points (P1, P2, and P3) have been identified as key locations for the study of floating platforms in ice-infested waters in the Baltic Sea. These locations are illustrated in Figure 3.5 and detailed in Table 3.1.
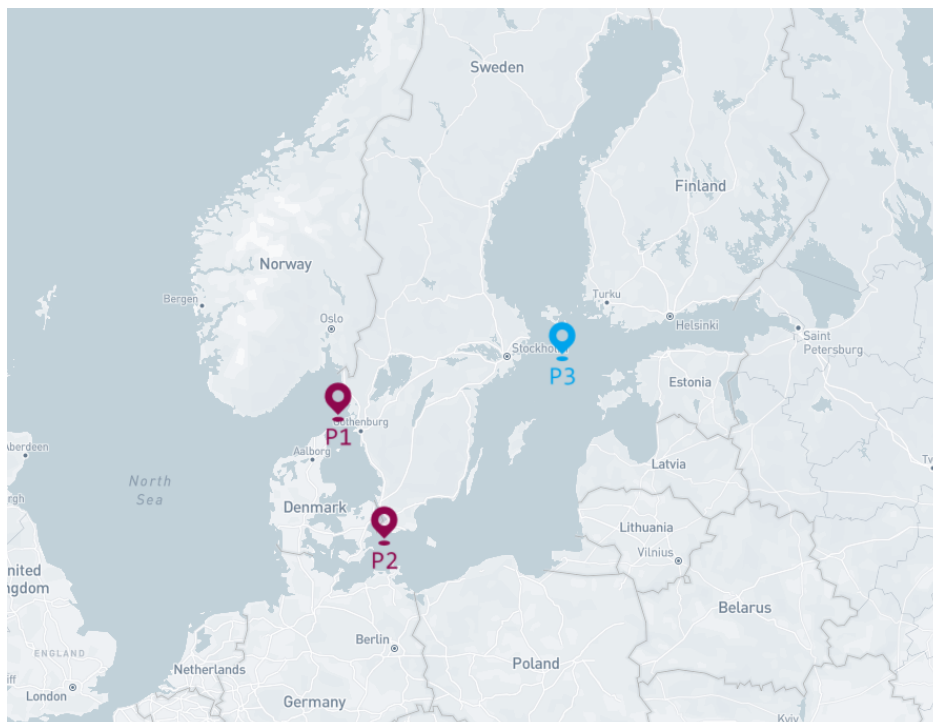
Figure 3.5: Map showing the locations of considered points (P1, P2, P3) in the Baltic Sea.

Table 3.1: Coordinates of considered points in the Baltic Sea

Point Name	P1	P2	P3
Longitude [deg.E]	11.03	12.97	20.43
Latitude [deg.N]	57.90	55.05	59.22

In selecting these locations, the primary focus was on regions where ice cover varies significantly, impacting the feasibility and design of floating platforms. The northern part of the Baltic Sea is known to be completely frozen during winter (Figure 3.6), particularly in the Bothnian Bay and the Gulf of Finland, presenting unique challenges for offshore wind projects [7]. Thus, P1, P2, and P3 were chosen to represent moderate ice conditions that allow for FOWF with minimal but significant impact on sea ice.

Point P1 (57.90° N, 11.03° E) is situated off the west coast of Sweden near Gothenburg. This location is characterized by its proximity to the Kattegat, which connects the Baltic Sea to the North Sea. The area experiences moderate wind speeds and is influenced by both marine and continental weather patterns. The proximity to major ports like Gothenburg makes it a strategic location for offshore wind projects [22].

Point 2 (55.05° N, 12.97° E) is situated in the southwestern part of the Baltic Sea. It is close to the Danish Island of Bornholm. Water is mostly shallow in this region and wind conditions are favorable for the installation of floating offshore wind turbines. This location has strategic importance because it is close to Denmark's energy infrastructure and existing floating wind turbines [23].

Point 3 (59.22° N, 20.43° E) is located in the northern side of the Baltic Sea. It is located south of Stockholm, Sweden. It's close to the Gulf of Bothnia and due to this, it has unique ice characteristics in the winter. This area was chosen because it's important to have an understanding of ice-structure interaction because of these unique ice conditions. Floating offshore wind turbines operating in this region will behave differently in the winter [24].

All locations were selected despite their actual water depths, which may not be the ideal depth for FOWTs. However, the primary goal of the thesis was to demonstrate the effect of ice conditions in those regions described above on the floating system.

3.4 Ice Formation and Types in the Baltic Sea

The Baltic Sea experiences significant seasonal ice cover, particularly in its northern parts, with variations in ice extent and thickness depending on the severity of the winter. Ice formation typically begins in the northernmost parts of the Bothnian Bay and extends to the Gulf of Finland by late October to early November. The Bothnian Bay, the Quark, and the Bothnian Sea generally freeze over completely during average winters, with the northern part of the Baltic Sea partially freezing. These reagions are deemed to be not economically feasibility for FOWT with current technologies at this stage.

Ice Formation Patterns

The ice formation and types in the Baltic Sea present significant challenges for offshore operations. The variations in ice cover and thickness, along with the types of ice encountered, necessitate comprehensive ice management strategies. Ice formation in the Baltic Sea can be classified into three categories based on the severity of the winter:

- **Mild Winter**: Characterized by a maximum ice cover of approximately 66,000 km^2. Ice forms mainly in shallow water areas of the Belts and Sounds. During mild winters, the ice thickness ranges between 10 cm to 15 cm. The sea is typically not completely covered, and ice cover is less than 6/10.

- **Average Winter**: The ice cover extends to about 204,000 km^2. The ice thickness increases to 30 cm to 70 cm, with the Baltic Sea and the Gulf of Finland largely frozen. Ice cover is more extensive, affecting navigation and marine activities more significantly.

- **Severe Winter**: During severe winters, the ice cover can extend up to 405,000 km^2. In such conditions, the Bothnian Bay, the Quark, and the Bothnian Sea are completely frozen, with ice thickness ranging from 30 cm to 70 cm. Ice can drift and accumulate, causing potential hazards for marine operations.

a) Mild winter
(1991 to 1992) —Maximum
extent of ice cover 66 000 km²

b) Average winter
(1961 to 1990) — Maximum
extent of ice cover 204 000 km²

c) Extreme winter
(1986 to 1987) — Maximum
extent of ice cover 405 000 km²
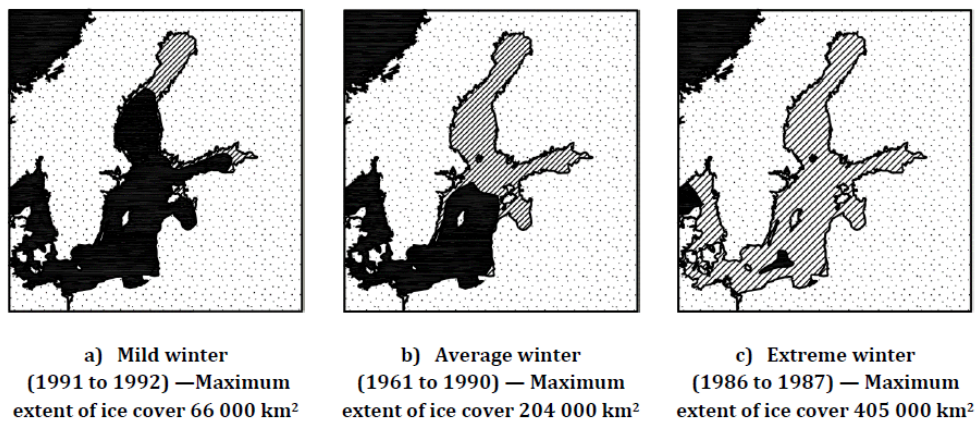
Figure 3.6: Ice formation and extent in the Baltic Sea during mild, average, and severe winters [7].

Ice Types Observed in the Baltic Sea

Several types of ice are commonly observed in the Baltic Sea, each presenting unique challenges for navigation and offshore operations:

- **Thaw Holes or Puddles**: These are common in the ice cover, especially as the ice starts to melt. Thaw holes indicate the weakening of the ice structure and the onset of melting.

- **Hummocked or Ridged Ice**: Formed due to the movement and pressure of the ice, creating raised structures. These ridges can be several meters high and pose significant obstacles to vessels and offshore installations.

- **Compacted Slush or Shuga**: Formed by the compression of brash ice, creating a

dense ice layer. This type of ice can be particularly challenging for propellers and underwater structures.

- **Rafted Ice**: Formed by the overlapping of ice floes, creating thicker and more stable ice formations. Rafted ice is more stable than other forms and can exert substantial pressure on structures.

The latter two types, compacted slush and rafted ice, are observed more frequently and for extended periods. These types are significant for the operational challenges they present, particularly in the fairways and harbors, where ice movement can obstruct navigation and impact offshore wind farm operations. As for the FOWT, the interaction of structure with ice ridges are concerning matter to look into details.

3.5 Ice Loads on Floating Platforms

3.5.1 Global Ice Load(Limiting Processes)

When evaluating ice events, it is important to consider various limiting processes such as limit stress, limit energy, and limit force. These processes must be examined to accurately assess the representative values of ice actions on structures[7].

Limit Stress Process: This occurs when ice failure adjacent to a structure (through compressive, shear, tensile, flexure, buckling, or splitting) dictates the ice action. Under limit stress conditions, the ice feature exerts sufficient force to fail and typically encompasses the structure. This is often the case in scenarios where ice actions are represented by typical values. For instance, ice floe splitting is a form of limit stress that can occur before the ice fully surrounds the structure.

Limit Energy Process: Also known as the limit momentum process, this occurs when the kinetic energy or momentum of the ice feature restricts the ice action. Examples include impacts from large isolated floes, ice islands, or icebergs, often seen in conditions such as old ice in summer.

Limit Force Process: This process is characterized by the inability of actions from winds, currents, and surrounding pack ice to cause ice failure against the structure. The ice feature in contact with the structure remains intact under these conditions.In some cases, a combination of these limiting processes might be applicable. When considering limit force processes, it should be ensured that the resulting action is less than that calculated using the limit stress process. Ice features can undergo splitting (limit stress process) within a limit force or limit energy scenario. For ice floes containing ridges, it is important to check limit stress conditions at the structure interface. Additionally, other failure processes should be examined for ridges and the interface between the ridge and level ice. Limit force actions associated with ridge building should be evaluated at the floe's edge. The ice action on the structure should be the minimum value derived from each of these processes. Typically, if multiple limiting processes occur simultaneously, the one producing the lowest ice action should govern the design and assessment.

3.5.2 Ice failure Mode

The mode of ice failure against a structure greatly influences the magnitude of the ice action. The failure mode for sea ice, whether it be crushing, shearing, flexure, or creep, is determined by factors such as ice thickness, the presence of ridges, ice velocity, ice temperature, and the shape of the structure.The geometry of a structure plays a crucial role in determining the ice forces it will experience. Key design aspects include the type of structure (such as multi-leg, monopod platform, or caisson) and the geometry at the waterline, whether vertical or sloping. Structures with vertical walls at the waterline typically encounter greater ice forces compared to those with sloping walls of similar dimensions. Sloping structures generally experience reduced ice forces, except when significant ice rubble accumulates on the sloped surface. When level ice or rafted ice interacts with a vertical structure, various failure modes can occur, with crushing being the most common for vertical configurations.
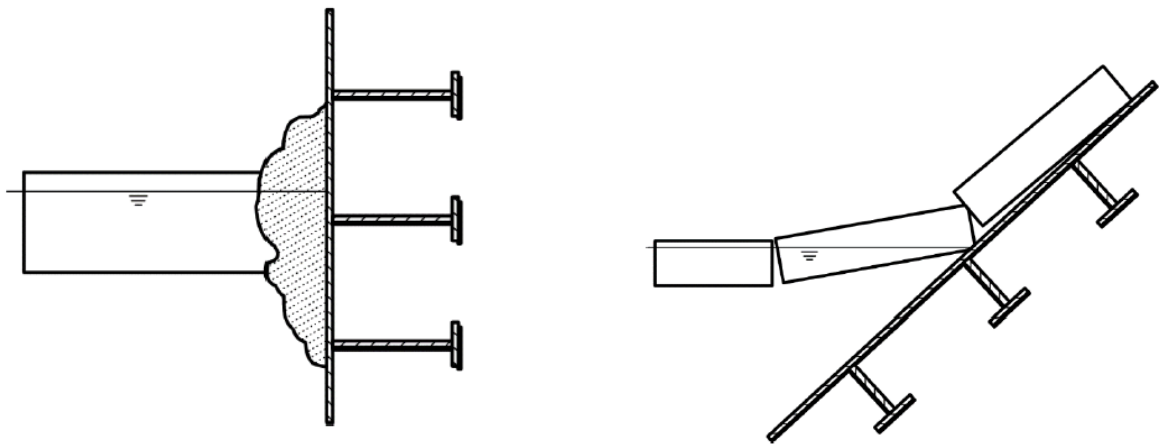
(a) Crushing Failure on Vertical structure[7]   **(b)** Bending Failure on Slope structure[7]

Figure 3.7: Ice failure modes on different geometry [7]

3.5.3 Global Horizontal Ice action due to crushing

$$F_G = p_G \cdot w \cdot h \tag{3.13}$$

where:

- F_G is the global horizontal crushing ice load, in megaNewtons (MN).
- p_G is the global average ice pressure, in megapascals (MPa).
- w is the width of the structure, in meters (m).
- h is the thickness of the ice sheet, in meters (m).

$$p_G = C_R \left\{ \left(\frac{h}{h_1} \right)^n \left(\frac{w}{h} \right)^m + f_{AR} \right\} \tag{3.14}$$

where:

- p_G is the global average ice pressure, in megapascals (MPa).

- w is the projected width of the structure, in meters (m).

- h is the thickness of the ice sheet, in meters (m).

- h_1 is a reference thickness of 1 meter.

- m is an empirical coefficient equal to -0.16.

- n is an empirical coefficient equal to -0.50 + $\frac{h}{5}$ for $h < 1.0$ m, and -0.30 for $h \geq 1.0$ m.

- C_R is the ice strength coefficient, in megapascals (MPa).

- f_{AR} is an empirical term given by:

$$f_{AR} = e^{\frac{-w}{3h}} \sqrt{1 + 5\frac{h}{w}}$$

3.5.4 Determination of Ice Strength Coefficient for the Baltic Region

The determination of the ice strength coefficient (C_R) for the Baltic region,requires adjustments to the ISO 19906 standard, which primarily addresses regions with heavy ice coverage annually. Since,this value does depend on the ice regime where longer and colder winter gives higher strength and more exposure to ice. In areas like the South Baltic Sea and Danish Straits, where heavy ice occurs only every 5 to 8 years, it is necessary to modify the C_R values accordingly [18].

According to the ISO 19906, the C_R value is determined by the return period of ice occurrence. For the danish Straits and baltic proper regions, empirical data and studies, such as those by Gravesen and Kärnä [20], provide a basis for these adjustments. The primary conclusion from these studies indicates that for the South Baltic Sea, $C_R^{SB} = 1.0$ MPa, whereas for the North Baltic, $C_R^{NB} = 1.3$ MPa for a 5-year return period.

Further adjustments based on frost indexes and ice coverage for the South Baltic Sea compared to the Swedish Kriegers Flak OWF area and Energy Island Baltic Sea Bornholm I and II OWF suggest safe usage of the C_R values derived from the reference study [19] and [18]. For a shorter return period (1-2 years), the study shows C_R values of 0.64 MPa, 0.98 MPa, and 1.05 MPa for return periods of 1, 50, and 100 years, respectively. Applying a combined velocity and safety factor of 1.2 and 1.11, the adjusted C_R values become 0.85, 1.3 and 1.4 for 1, 50 and 100 years, respectively, return period.

This method ensures that the ice strength coefficient is appropriately adjusted for the specific ice conditions of the Baltic region, providing a reliable basis for structural design in offshore wind farms.

3.5.5 Ice Ridge(Limit Stress Mechanism)

In regions with first-year (FY) ice, such as the Baltic Sea, ice ridges often represent the critical ice events impacting structural designs. These ice ridges are complex formations composed of various elements that collectively contribute to the loads exerted on offshore structures. Typically, an ice ridge consists of a sail above the waterline, a consolidated layer formed from

re-frozen multiple thinner ice sheets, and a keel made up of partly consolidated or loose ice blocks (see Figure 3.8). The formation of these ridges can result from nearshore effects, ice packing due to wind and current actions, or the blocking effect of offshore structures, which can cause ice to accumulate and form ridges.
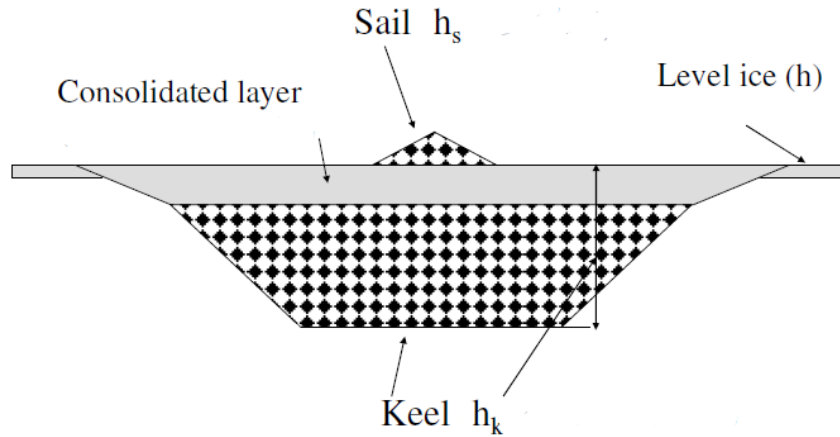
Figure 3.8: Schematic representation of an ice ridge showing the sail, consolidated layer, and keel.[17]

For the Danish Strait and Baltic Proper regions, ice ridges can form from any direction due to the presence of nearby wind farms and the turbine foundations themselves. This formation mechanism makes it essential to understand the composition and behavior of these ice ridges. Ice engineering often relies on limited field measurements from areas with severe sea ice conditions, and standards may include broad estimates without defining precise uncertainties and probabilities. Therefore, for the Baltic South, where sea ice is moderate, it is crucial to select design parameters carefully. Key parameters include the basic ice thickness, the assumed thickness of the consolidated layer, and the maximum size of ice floes. These parameters should follow recommendations from standards such as ISO 19906 [7], ensuring they are robust enough to withstand local ice conditions.

Estimating the properties of ice ridges involves analyzing data from similar wind farms in the southwestern Baltic Sea, where conditions are representative of the Swedish Kriegers Flak OWF area. Ice ridge formation when it starts include ice volume in the keel and sail combined, and this ice has the potential to refreeze and get rafted. As the blocks of ice attain water temperature, keel ice blocks can experience slight freezing because of negative heat release. But it depends on the temperature of the ice sheet which forms the ridge. The process completes with the formation of firm ice layer on the top as heat is released from surface to the cold air above it.

The consolidated layer typically has a porosity of about 30 %, and freeze front progresses faster than in the original level ice. This results in the consolidated layer being thicker than the surrounding level ice. These values and relationships for ridge morphological parameters have been studied extensively in various regions. For regions like Baltic Proper South, using field data from areas with similar ice conditions is recommended.

3.5.6 Ice Ridge Loads Calculation

The ice ridge loads can be calculated according to ISO 19906 [7] or IEC codes [13].

An accurate, theoretical determination of the actions caused by ice ridges is difficult. An upper bound estimation of the horizontal action caused by a FY ridge, F_R, can be obtained as given by Formula 3.15 [7]:

$$F_R = F_c + F_k \tag{3.15}$$

where

- F_c is the action component due to the consolidated part of the ridge;
- F_k is the keel action component.

Since the volume of the sail is small compared to that of the keel, the effects of the ridge sail can be neglected in the case of FY ridges.

There are several models available to calculate the unconsolidated keel action component F_k. Typically, passive failure models are employed to estimate the keel action component on vertical or inclined structures. Observations show that keel cohesion tends to range from zero at the base of the keel to a maximum just below the consolidated layer. Given these conditions, the keel action on vertical structures can be calculated using a modified approach, as outlined in equations 3.16 and 3.17.

$$F_k = \mu_p h_k w \left(\frac{h_k \mu_p \gamma_e}{2} + 2c \right) \left(1 + \frac{h_k}{6w} \right) \tag{3.16}$$

$$\mu_p = \tan \left(45° + \frac{\phi}{2} \right) \tag{3.17}$$

where

- μ_p is the passive pressure coefficient;
- ϕ is the angle of internal friction;
- c is the apparent keel cohesion (an average value over the keel volume should be used);
- w is the width of the structure;
- γ_e is the effective buoyancy, in units consistent with c.

The effective buoyancy is given by Formula 3.18:

$$\gamma_e = (1 - e)(\gamma_w - \rho_i)g \tag{3.18}$$

where

- e is the keel porosity;
- γ_w is the water density;
- ρ_i is the ice density.

The results of the ice ridge estimation for all three locations are discussed in the section **??**.

3.5.7 Ridge-Building Load (Limit Force Mechanism)

To calculate the ice actions resulting from ridge building, two primary parameters are required as inputs. One is the ridge-building action per unit length, P_D, on the back of the ice floe, and the other is the width of the ice feature, D, over which the pack ice accumulates. The limit ridge-building action can be determined by using Equation 3.19:

$$F_D = P_D \cdot D \tag{3.19}$$

(a) Ridge-building action for thick floe [7]

(b) Ridge-building action for consolidated ridge [7]
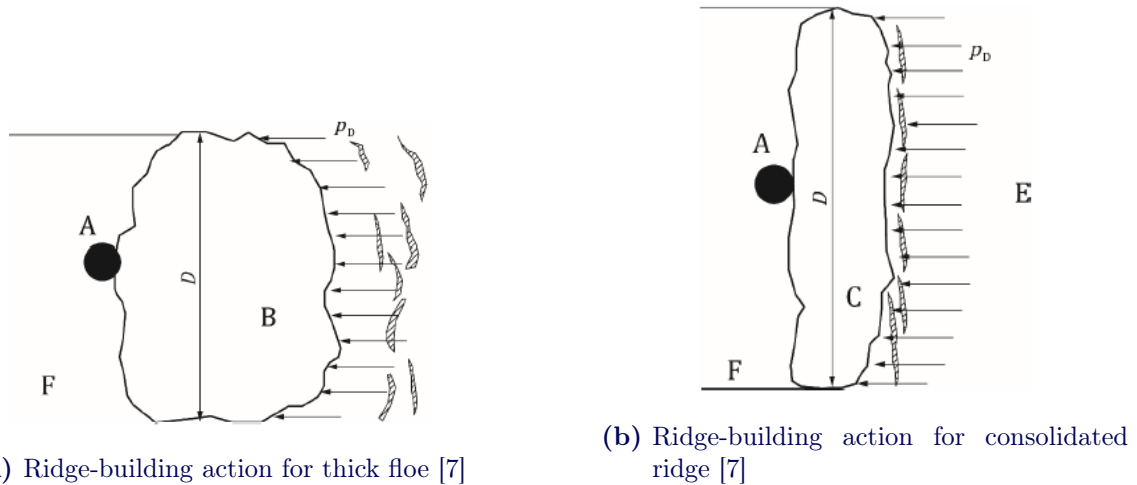
Figure 3.9: Ridge-building action behind thick floe or ridge (Limit Force Mechanism)

Key:

   A Structure

   B Thick ice floe

   C Thick consolidated ice ridge

   D Width of the ice feature, expressed in meters

   E Surrounding ice sheet

   F Open water in wake of structure and ice feature

  p_D Line action imposed on the width of the ice feature

Observations indicate that ridge building and ice rubble formation in front of structures primarily result from the ice bending and falling out-of-plane. This phenomenon was initially studied in the 1980s and 1990s in the Beaufort Sea, revealing that ridge-building events commonly occur when thinner ice features encounter thicker, embedded ice features within the pack. These interactions can induce significant horizontal forces, necessitating rigorous design considerations to maintain structural integrity.

A general expression for the ridge-building action is given by Equation 3.19:

$$p_D = p_{D0} \left(\frac{h_0}{h} \right)^{1.25} \tag{3.20}$$

where p_{D0} is the ridge-building action per unit width for a reference ice thickness h_0, and h is the thickness of the ice floe or ridge in meters.

Figure 3.10 shows a collection of measured data points on ridge-building actions. All data are derived from ridge-building events where ice floes collided with thicker ice features. These data include values from scenarios where thicker ice features were embedded in the pack, sourced from various studies (References [148], [149], and [150]). The measured data points are displayed in relation to the normalized ridge-building actions per unit width given by the ratio of p_D to p_{D0}.
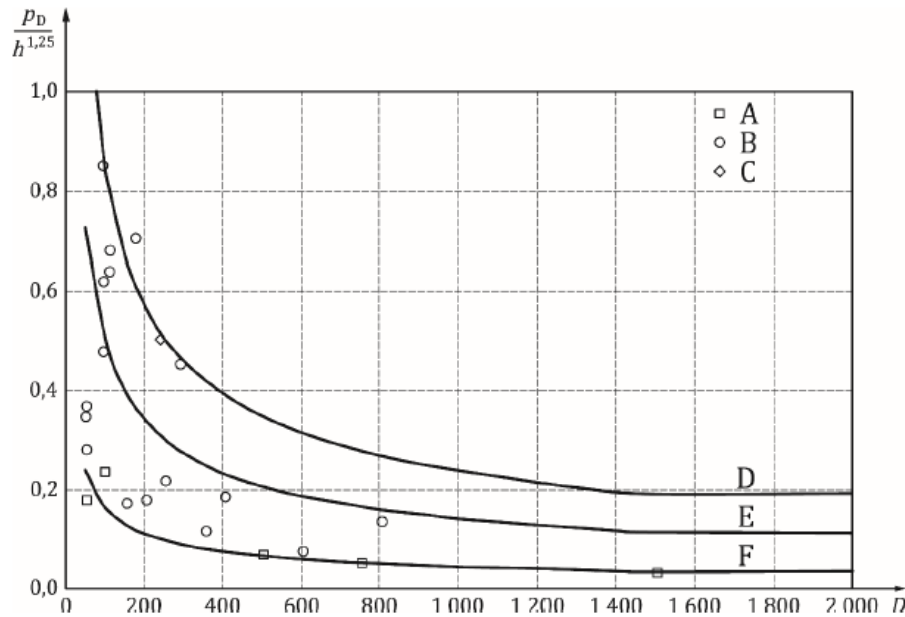
Figure 3.10: Ridge-building actions versus width normalized to unit thickness of first-year ice (raised to the power of 1.25). [7]

The review of measured data indicates that for ridge building and ice rubble accumulation, a uniform distribution of the normalized ridge-building actions is suggested, particularly for ice features with widths greater than 300 meters. For narrower features or ice floes frozen into the pack, more precise modeling is required to account for the increased complexity and variability in the ice interactions.

The estimated uncertainty factors in the determination of ridge-building actions, based on measured processes, range between 1.5 and 2.0 for deterministic calculations. For conventional design scenarios, an uncertainty factor of 1.5 is recommended for ridge-building actions, ensuring the design remains conservative and reliable in varying conditions.

3.5.8 Blockage Effect

Ice jamming, also known as the blockage effect, is a significant concern for offshore wind turbine structures, particularly those with multi-leg configurations. When the ratio of the clear distance between the legs (L) to the width of the legs (w) is less than 5 according to ISO19906 [7], ice can accumulate between the legs, leading to increased ice loads. This effect can significantly impact on the system and can lead to the failure of the floater.

The reference FOWT is the semisubmersible floater type four cylindrical column , Hence, analyzing the chance of ice jamming is particularly relevant. In this thesis, both jammed and unjammed ice conditions are considered and the loads on the legs are estimated. The analysis includes assessing individual leg loads and the global load on the structure.

The global loads on legs are calculated using the following equation from the Arctic offshore engineering book [17]:

$$\text{Global load} = \text{Individual leg load} \times \text{Number of legs} \times \text{Leg factor} \qquad (3.21)$$

The leg factor is influenced by the direction of ice movement and the spacing between the legs. For example, in a four-legged structure, the leg factor can range from 0.5 to 0.9 based on spacing and interaction effects. Experimental data and computational models, such as those by Wang et al., have shown that for widely spaced legs, the leg factor can approach 1. In this model, a value of 0.7 is used for four legs.The calculations for the ice blockage effect are presented detials in the section 4.1.4.

The blockage effect is more pronounced with first-year ice ridges (FY ridges), where ice rubble in the keel can significantly impede the motion between the legs.

The diagrams and calculations for the selected model illustrate the impact of ice jamming on the wind turbine structure. Without blockage, the individual leg loads at Point 1,2, and 3 include factors like the global leg crushing load and keel load. However, when effective blocked width is considered, the loads significantly increase. For instance, the blocked width, calculated as 90.13, leads to a substantial rise in global leg loads, with the global leg keel load at P2 increasing to 82.2 MN and the total load reaching 121.6 MN.

To mitigate the risk of ice jamming, several design suggestions can be implemented. These include increasing the spacing between the legs to achieve a higher L/w ratio, thereby reducing the likelihood of ice accumulation. Additionally, incorporating design features that minimize ice interaction, such as sloped surfaces or ice-breaking structures, can help manage ice loads more effectively.

In summary, addressing ice jamming in the design and analysis of offshore wind turbines is essential to ensure structural resilience and operational reliability. The use of standards and guidelines, such as those outlined in ISO 19906 and DNV GL, provides a framework for mitigating these risks through careful consideration of ice loads and structural design adjustments. By implementing these strategies, the potential adverse effects of ice jamming can be minimized, enhancing the overall performance and safety of offshore wind turbines.
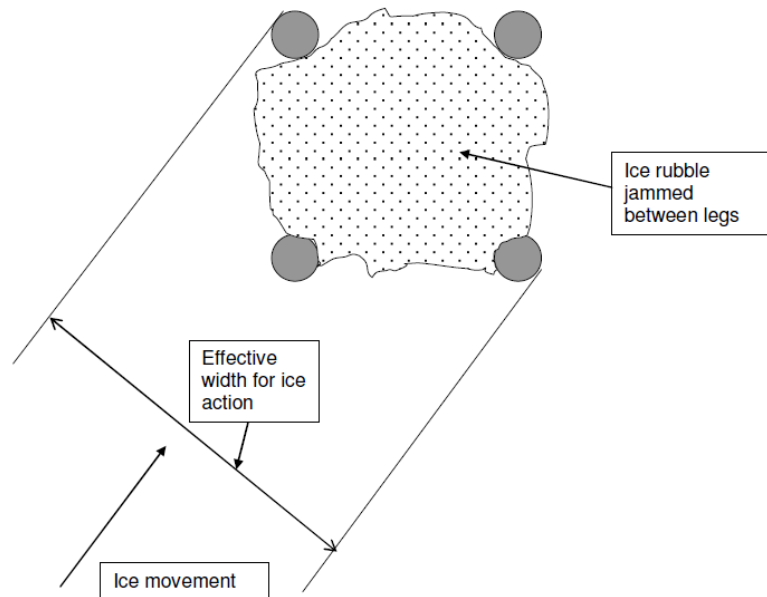
Figure 3.11: Increase in effective width due to ice blocking on a multi-leg structure[17]

3.6 UMaine VolturnUS-S 15-Megawatt Offshore Reference Wind Turbine Model

3.6.1 UMaine VolturnUS-S Semisubmersible Platform Model

The reference platform discussed in this report which is the open source floater widely used in the academic and research projects, is a steel semisubmersible structure with four columns. Table 3.2 provides the general properties of the platform,such as masses, dimensions, buoyancy, and inertias. Figure 3.12 illustrates the layout of the hull, which consists of three 12.5-m-diameter buoyant columns arranged radially with centers spaced 51.75 m apart from the tower's vertical axis [37]. A fourth buoyant column, positioned at the center of the platform, supports the platform-tower interface in the surge-sway plane. This central column connects to the outer columns via three 12.5-m-wide by 7.0-m-high rectangular bottom pontoons and three 0.9-m-diameter radial struts attached at columns top.

When on station, the total mass of the platform is 17,854 t, with 3,914 t being structural steel and 2,540 t comprising fixed iron-ore-concrete ballast, distributed equally at the bases of the three radial columns. Additionally, 11,300 t of seawater ballast is used, filling the majority of the three submerged pontoons. The tower interface has a mass of 100 t and connects to the freeboard located 15 m above the waterline, assumed to be rigidly connected to the substructure [37].

Table 3.2: Semisubmersible Platform Properties

Parameter	Units	Value
Hull Displacement	m^3	20,206
Hull Steel Mass	t	3,914
Tower Interface Mass	t	100
Ballast Mass (Fixed/Fluid)	t	2,540/11,300
Draft	m	20
Freeboard	m	15
Vertical Center of Gravity from SWL	m	-14.94
Vertical Center of Buoyancy from SWL	m	-13.63
Roll Inertia about Center of Gravity	kg-m^2	1.251E+10
Pitch Inertia about Center of Gravity	kg-m^2	1.251E+10
Yaw Inertia about Center of Gravity	kg-m^2	2.367E+10

The system's hydrodynamic properties are represented in OpenFAST's hydrodynamics module, HydroDyn, using a potential flow model augmented with a quadratic drag model. For this section, all values refer to the platform's reference point, defined in OpenFAST as the intersection of the SWL and the tower axis. Frequency-dependent coefficients for the potential flow model were computed using the boundary-element-method hydrodynamics solver WAMIT v6, addressing the first-order hydrostatics, diffraction, and radiation problems. The resulting response amplitude operators (RAOs) were then used to compute second-order wave-excitation quadratic transfer functions (QTFs) [5]. These pre-calculated data from the reference document [37] were used as input for dynamic simulations in the Orcaflex software. In summary, the WAMIT coefficients account for the platform's hydrodynamic added mass, wave-radiation damping, hydrostatic restoring, and first-order and second-order wave excitations.
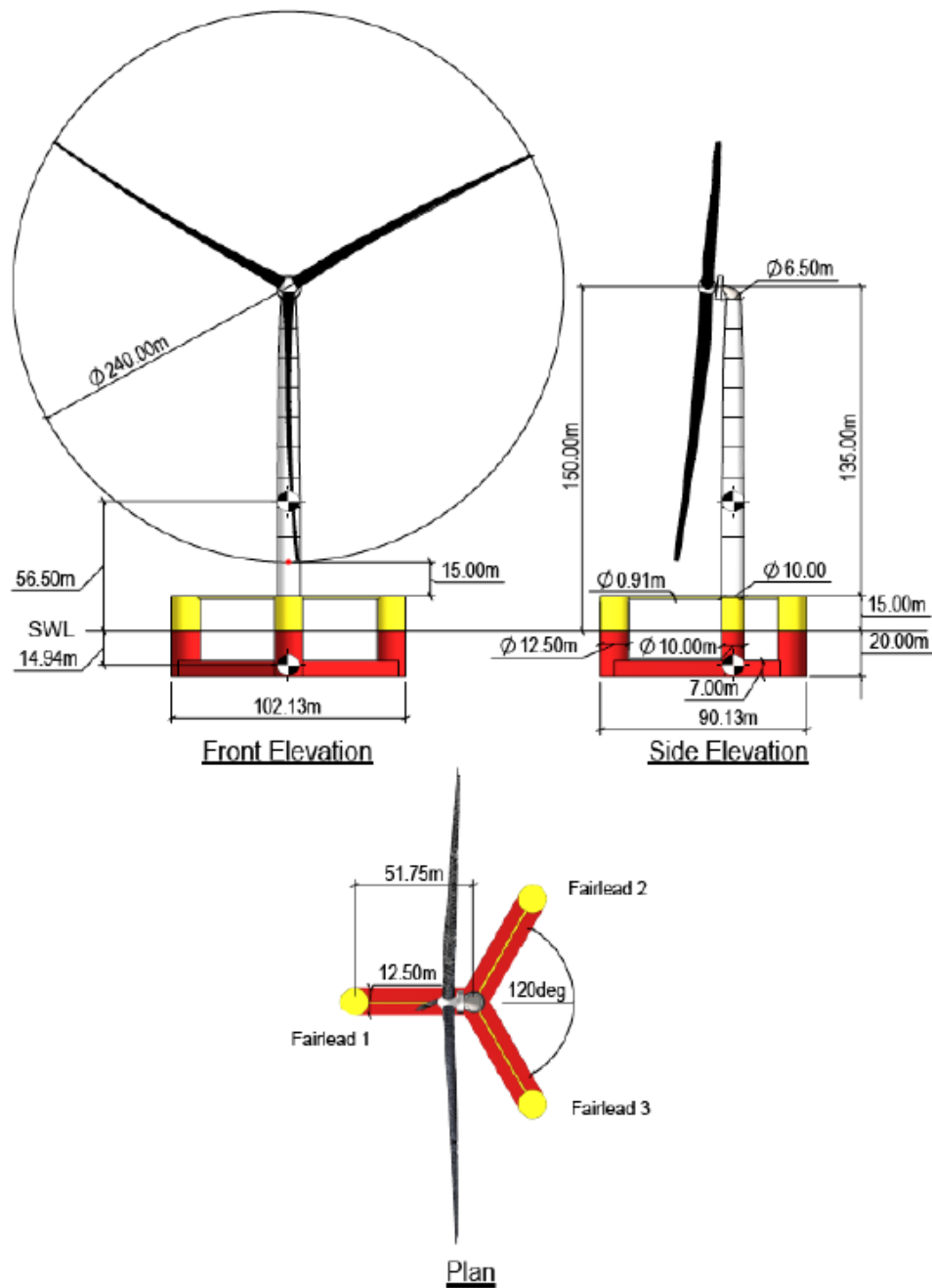
Figure 3.12: Arrangement of the UMaine VolturnUS-S semisubmersible platform hull.

3.6.2 Mooring System Properties

This section describes the design of the reference chain mooring system. The properties and arrangement of the mooring system are detailed in Table 3.3 and Figure 3.13[37]. The configuration includes three 850-meter-long chain catenary lines, each connected at the fairlead to one of the platform's three outer columns at a depth of 14 meters below the SWL. The lines extend radially to anchors spaced equally at 120 degrees in the surge-sway plane, positioned at a depth of 200 meters and spaced radially 837.6 meters from the tower's centerline. All lines utilize an R3 studless chain with a nominal (bar) diameter of 185 millimeters (mm). Table 3.4 lists the mooring line drag and added mass coefficients, selected with reference to

DNVGL-RP-C205 (Det Norske Veritas 2010) and DNVGL-OS-301 (DNV GL 2015). These given information were extracted from the reference model [37] and utilized as input in the simulations.

Table 3.3: Mooring System Properties

Parameter	Units	Value
Mooring System Type	-	Chain Catenary
Line Type	-	R3 Studless Mooring Chain
Line Breaking Strength	kN	22,286
Number of Lines	-	3
Anchor Depth	m	200
Fairlead Depth	m	14
Anchor Radial Spacing	m	837.6
Fairlead Radial Spacing	m	58
Nominal Chain Diameter	mm	185
Dry Line Linear	kg/m	685
Extensional Stiffness	MN	3270
Line Unstretched Length	m	850
Fairlead Pretension	kN	2,437
Fairlead Angle from SWL	-	56.4

Table 3.4: Mooring Line Drag and Added Mass Coefficients

Mooring Line Coefficients	Relative to Chain Nominal Diameter	Relative to Volume-Equivalent Diameter
Normal Added Mass	1	0.82
Tangential Added Mass	1	0.27
Normal Drag	2	1.11
Tangential Drag	1.15	0.20
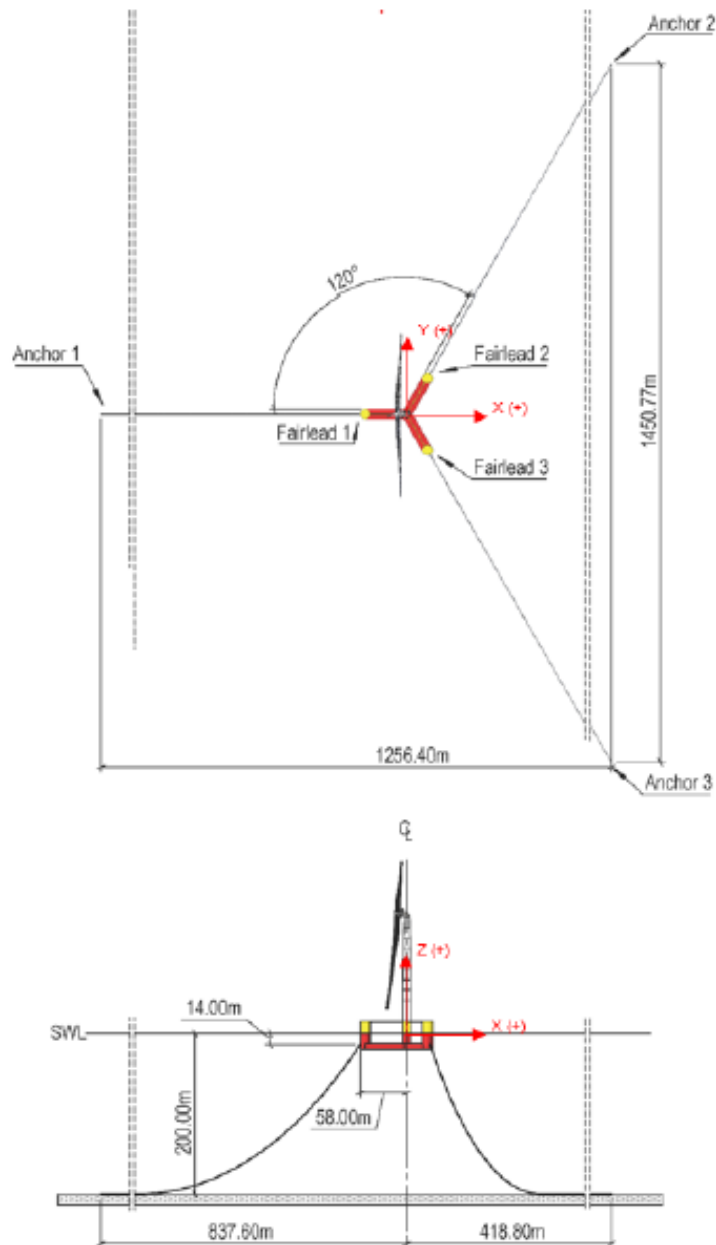
Figure 3.13: Arrangement of the UMaine VolturnUS-S semisubmersible platform mooring system.

3.7 Design Load Analysis on the floating Platforms

3.7.1 Design Load Cases

The estimated ice loads shall be evaluated for various environmental conditions such as design loadcases as mentioned in DNV [8]. For the design load cases (DLC) 9.1 to 9.5, associated with drifting sea ice conditions, the following scenarios require thorough examination:

DLC 9.1 involves assessing the structural integrity of the offshore wind turbine under conditions representing a 50-year recurrence of sea ice during power production. In DLC 9.2, the focus shifts to evaluating the dynamic ice loads associated with the expected history of

Table 3.5: Load Factors for Design Loadcases

Load factor Set	Limit state	Load categories (Environmental)
a	ULS	1.35
b	ULS for abnormal wind cases	1.1

moving ice. Similar evaluations are necessary for DLC 9.3 and DLC 9.5, where the wind turbine's response during periods of standstill or idling is considered.

In DLC 9.4, the analysis extends to include the impact of hummocked ice and ice ridges during idling. The loads from these ice features are treated as quasi-static, given that the significant rubble mass is presumed to provide sufficient damping to negate any dynamic effects. Furthermore, dynamic interactions between the wind turbine structure and moving sea ice are accounted for using a dynamic magnification factor of 1.5, particularly relevant for floating turbines [10, 7]. The quasi-static assumption for ice ridges is due to the large rubble mass's capacity to dampen potential dynamic responses, allowing for a simplified analytical approach.

In addition to the conditions associated with drifting sea ice, the design load cases (DLC) 1.6 and 6.1 should be considered as reference scenarios. Specifically in DLC 1.6, the offshore wind turbine must be evaluated under the assumption of experiencing severe sea state conditions during operation. For DLC 6.1, where the wind turbine is parked and either in standby mode or idling, the analysis should incorporate a turbulent wind model alongside irregular sea state conditions. In this context, either the 50-year recurrence significant wave height or the 50-year recurrence mean wind speed, or a set of values with a joint recurrence period of 50 years, should be utilized. The load analysis were carried out incorporating all the environmental conditions as mentioned in the table, and ice loads are applied using the partial safety factor as recommended by the DNV rule [11].

The ice loads are calibrated by using the partial safety factor method which is a design approach that ensures structural safety by applying specific factors to account for uncertainties in loads and material strengths. This method uses characteristic values, representing typical extreme conditions, to determine these factors. Load factors are adjusted to consider potential deviations, simultaneous load exceedances, and uncertainties in modeling and analysis. By incorporating these factors, the method ensures that structures can withstand unfavorable conditions, maintaining safety and reliability. This approach is crucial for designing structures that remain safe under various unexpected scenarios [7, 10, 11].

Table 3.6: Table of Design Loadcases for Drifting Sea Ice Conditions

Design Situation	DLC	Wind Condition	Waves	Wind and Wave direction-ality	Sea Cur-rent	Water Level	Ice Condition	Type of Analy-sis	Partial Safety Factor
Drifting sea ice, Power Production	1.6	NTM, $V_{in} < V_{hub} < V_{out}$	SSS, $H_s = H_s$,SSS	COD, UNI	NCM	NWLR	no ice	ULS	N
	9.1	NTM, $V_{in} < V_{hub} < V_{out}$	no wave	COD, UNI	NCM	NWLR	Ice load in horizontal direction from moving ice at relevant velocities. $h = h_{50}$ or largest value of moving ice Dynamic effects from ice loading – frequency lock-in effects	ULS	N
	9.2	NTM, $V_{in} < V_{hub} < V_{out}$	no wave	COD, UNI	NCM	NWLR	Ice load in horizontal direction from moving ice at relevant velocities Use values of h corresponding to expected history of moving ice occurring Dynamic effects from ice loading – frequency lock-in effects	ULS	F/N
Drifting sea ice, Parked	9.3	Turbulent - EWM, $V_{hub} = V_1$	no wave	COD, UNI	NCM	NWLR	Pressure from hummocked ice and ice ridges	ULS	N
	9.4	NTM, $V_{hub} < 0.7V_{50}$	no wave	COD, UNI	NCM	NWLR	Horizontal load from moving ice at relevant velocities Use values of h corresponding to expected history of moving ice occurring Dynamic effects from ice loading – frequency lock-in effects	ULS	F/N
	9.5	Turbulent - EWM, $V_{hub} = V_1$	no wave	COD, UNI	NCM	NWLR	Horizontal load from moving ice at relevant velocities. $h = h_{50}$ or largest value of moving ice Dynamic effects from ice loading – frequency lock-in effects	ULS	N
	6.1	EMW, $V_{hub} = V_{ref}$	ESS, $H_s = H_{s,50}$	MIS, MUL	ECM, $U = U_{50}$	EWLR	no ice	ULS	N

3.7.2 Dynamic Analysis in Orcaflex

OrcaFlex is designed to model and analyze large rigid bodies, like ships, floating platforms, barges, TLPs, or semi-submersibles, where wave diffraction effects are significant. For these structures, the vessel's motion is determined using Response Amplitude Operators (RAOs), Quadratic Transfer Functions (QTFs), and other data obtained from diffraction analysis. This detailed hydrodynamic information is often generated using the diffraction analysis using a potential solver software such as Orcawave and then imported into OrcaFlex [31].

3.7.2.1 Floater Modelling in Orcaflex

Modeling a floater in OrcaFlex involves creating a detailed mathematical representation of the floater. In Orcaflex, floater is modelled as a vessel object. Its properties are defined such as Mass and moment of inertia, Load and displacement RAOs, stiffness, added mass and damping matrix for every combination of wave periods and wave directions. Also the initial

position is defined in vessel(floater) data form. Then, applied load on the floater due to ice is also modelled. This included the direction, position, and magnitude of the load. A typical vessel data form is shown in figure 3.14.
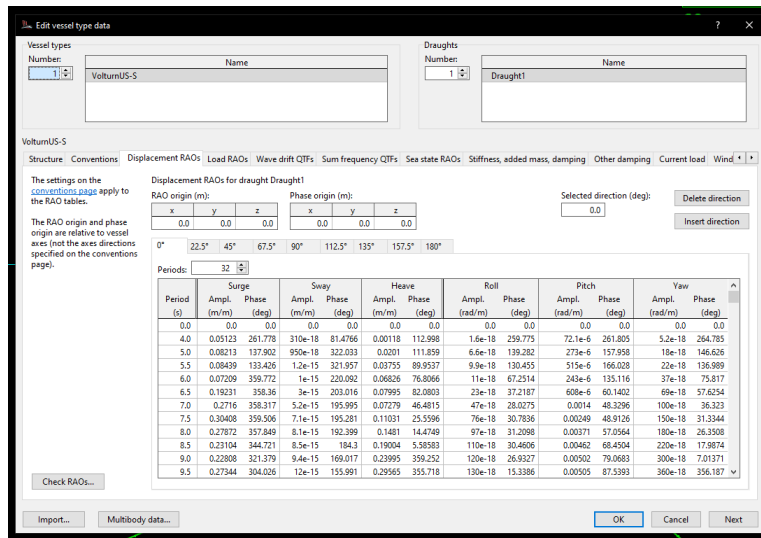
Figure 3.14: Input Vessel Data

3.7.2.2 Mooring system modelling in Orcaflex

In OrcaFlex, the mooring lines are modeled as line objects. The line type is defined and all the relevant data is input for the mooring lines in Orcaflex line type menu. The line type for mooring line is in general category. In line type data form, Line diameter, mass per unit length, bending stiffness, normal and axial drag coefficients, normal and axial lift diamter, added mass coefficient, seabed friction coefficient, stress loading factor, contact diameter and length is defined. Apart from it, end connection of both ends of each mooring line is defined. Their initial positions are defined. Mooring line data form and menu for definition of different line types in orcaflex is shown in figure 3.15 and 3.16

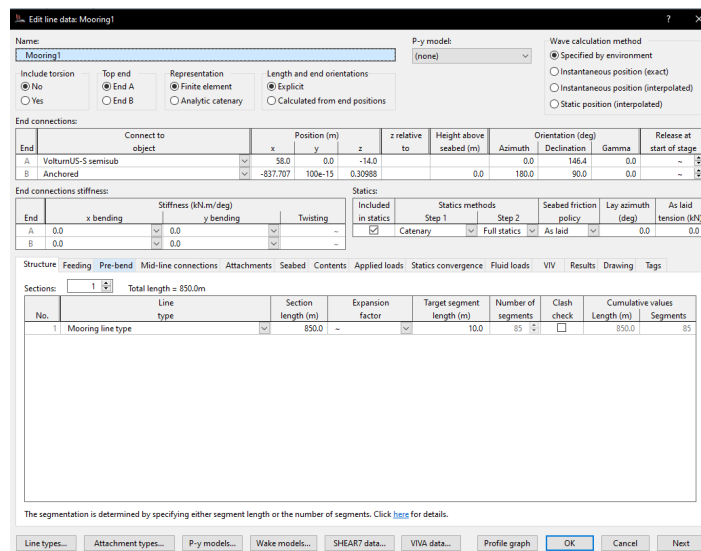**Figure 3.15:** Mooring line data form in Orcaflex.
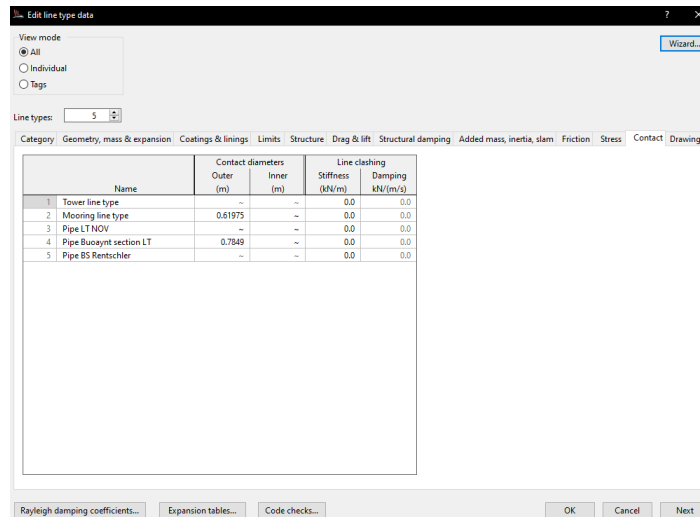
Figure 3.16: line data types form in Orcaflex.

3.7.2.3 Tower modelling in Orcaflex

In OrcaFlex, tower is modeled using line object. The line type is defined and all the relevant data is input for the tower in Orcaflex line type menu. The line type for tower is in homogeneous pipe category. In line type data form, outer and inner diameters are defined. As each tower section has different diameter in reality, so 20 different sections are defined in orcaflex and for each of these sections, outside and inside diameter is given to properly represent tower as a line object. Moreover, youngs modulus, mass per unit length, bending stiffness, normal and axial drag coefficients, added mass coefficient, seabed friction coefficient, stress loading factor, and length is defined. Apart from it, end connection of both ends of tower is defined. Their initial positions are defined. Tower line data form and tower diameter definition page is shown in figure 3.17 and 3.18

Figure 3.17: Tower line data form in Orcaflex.

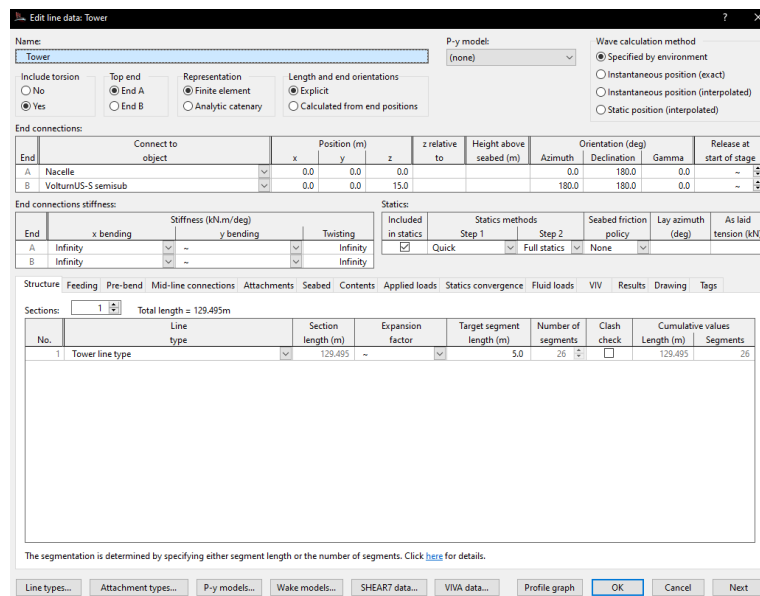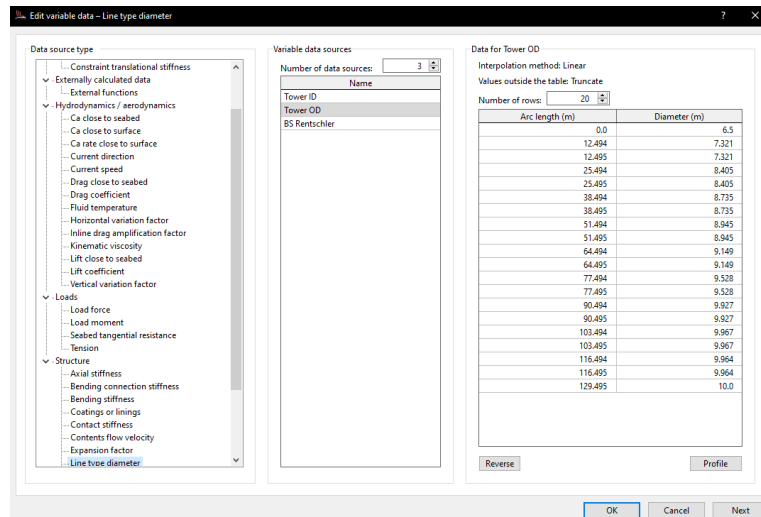**Figure 3.18:** Tower diameter definition form in Orcaflex.

3.7.2.4 Specification of Environmental Loads in Orcaflex

After setting up the models and input data for the load analysis, the environmental conditions to which the system is subjected,are modelled in Orcaflex for the different design loadcases DLC mention in 3.6 in all the considered points (P1, P2 and P3), in order to simulate the dynamic analysis in the realistic sea state conditions.

The **environment** defines the conditions to which objects in the model are subjected; it consists of the sea kinematic viscosity, temperature, water density, seabed type, sea depth, current direction and speed, wave height, wave peak period, wave direction, wave γ, and wind direction and speed. These components are illustrated in the figure below, which depicts a global coordinate system with axes X, Y, and Z. The Z-axis represents the vertical direction, with the still water surface, datum current direction, and wave direction indicated. The Y-axis is aligned horizontally, while the X-axis represents the horizontal plane. Additionally, the seabed's origin and the direction of the slope are defined. All environmental conditions, including currents, wind, and wave directions, are specified relative to these global axes [30, 32].
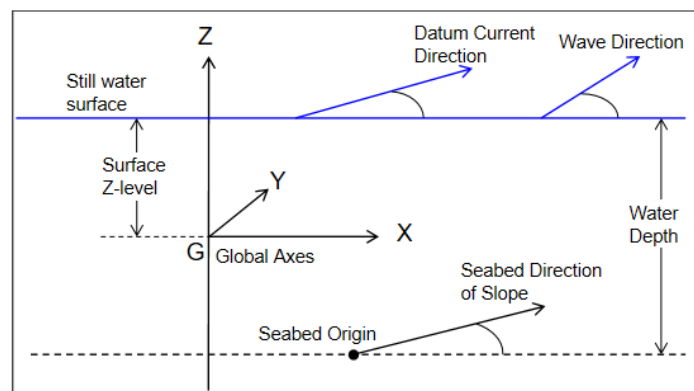
Figure 3.19: Environmental conditions and global axes in offshore models [30].
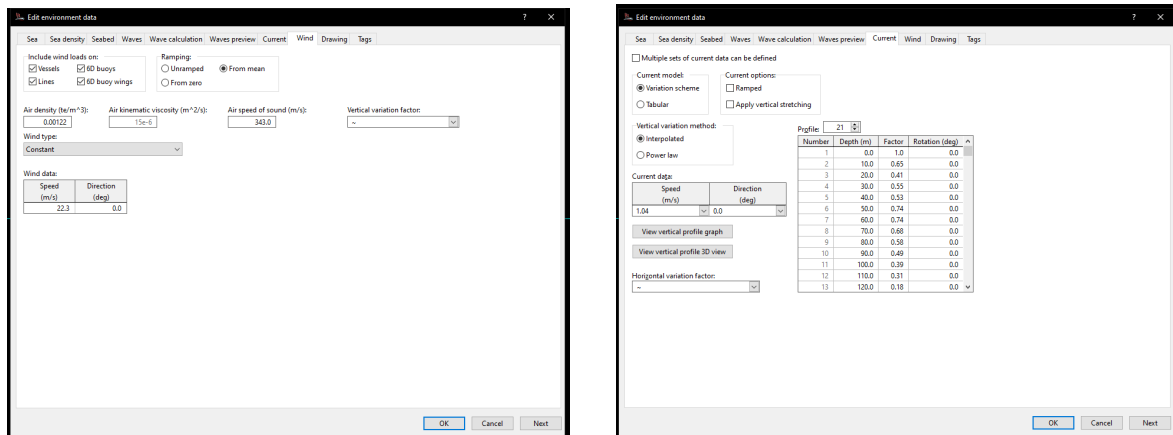
Figure 3.20: Input Environmental data in orcaflex

After complete modelling in Orcaflex, the model is ready to be simulated. The 3D, shaded view, of the model can be seen in 3.21.
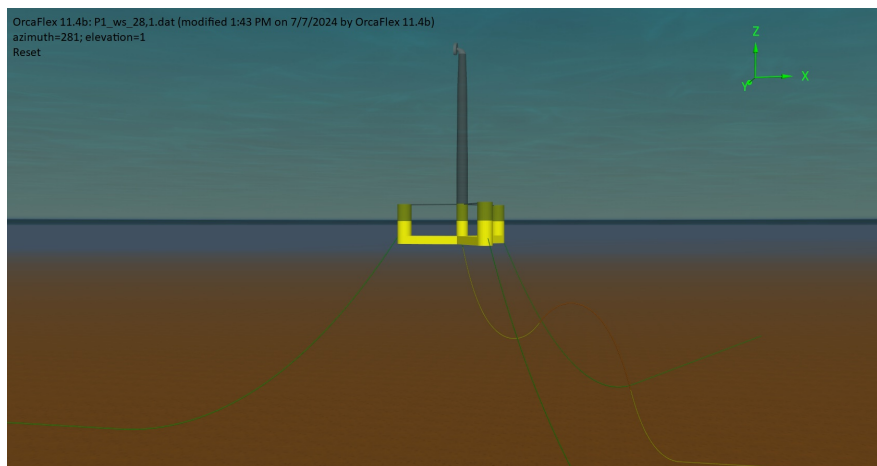
Figure 3.21: Orcaflex Model of the UMaine VolturnUS-S semisubmersible platform and mooring arrangement.

3.8 Ice Mitigation Strategies

Floating platforms in ice prone area encounter more complex and significant challenges due to various ice loads and events. In practice, the effective ice mitigation strategies are employed for worst case conditions for ensuring the platform's safety and operational integrity. Despite the challenges, there are a few interesting perspectives for the FOWT in icy environment[7].

A. Passive Systems

Effective passive systems can involve configuring the structure to endure the extreme ice forces without active IM system. This approach involves configuring the structural designs to withstand the observed ice conditions. IM strategies from O & G and BFOW can be applied to the system.

B. Semi-Passive Systems

Semi-passive systems imply the physical IM but moving and disconnecting the platform to avoid ice are not part of the approach. This system is used in the region with less frequent ice conditions.

C. Semi-Active Systems

This approach is mainly used for seasonal platform where the physical IM system is not being practised. The structure is pulled away from the zone where the ice loads can be critical. This system usually equipped with ice alert sensors.

D.Active Systems

Active systems include disconnection or relocation of the structure to mitigate the impact of severe ice conditions. The active system is also supported by continuous monitoring system to identify the ice threats. When there is a severe environmental conditions or ice events, the floater can stop all the operations, disconnected and relocated to the safe area. Figure 3.23, demonstrates all the IM system configurations for floating systems in ice-infested waters.

An effective ice mitigation strategy for floating platforms integrates robust structural design, active and passive ice management systems, and comprehensive monitoring. Regular updates to the plan are necessary as new technologies and ice behavior data become available. Moreover there are more new ice management equipment such as submerged bubbler systems and flow inducers for floating platforms and offshore wind energy systems, as detailed in Marina Dock Age [33].

Flow inducers are electric-powered propellers which can generate water flow under the ice layer and can make the large ice-free area around the platforms. They claim to be cost-effective with low capital cost and easy to maintain. They can be powered by the electricity generated by the turbines. By installing temperature sensors to reduce the energy consumed by the device and turning them off when not needed.[33]. Another approach is by installing secondary sloped structure such as ice cones at the waterline area. The detail of the measures is presented in the next section 3.8.1.
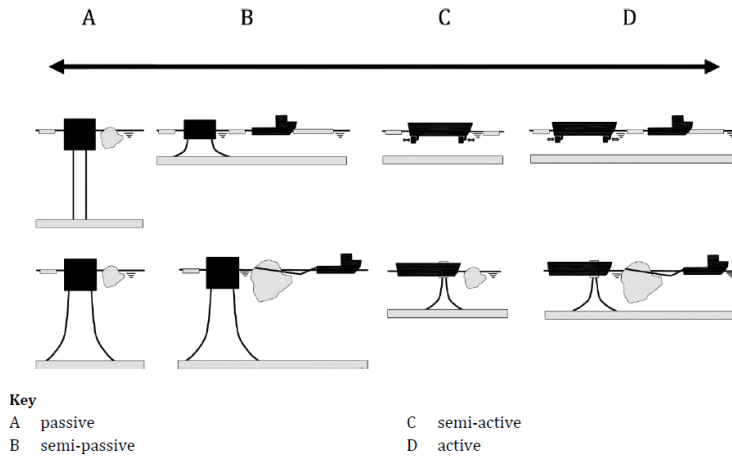
Figure 3.22: Various IM systems for icy waters[7].

3.8.1 Constructive Ice Measures(Ice Cones)

The utilization of an ice cone, or sloped structure, in offshore wind turbine foundations is an effective strategy to mitigate ice loads. The primary objective is to manage the interaction between ice and the structure by causing the ice to bend and break or ride up along the slope, thereby reducing the forces exerted on the structure.
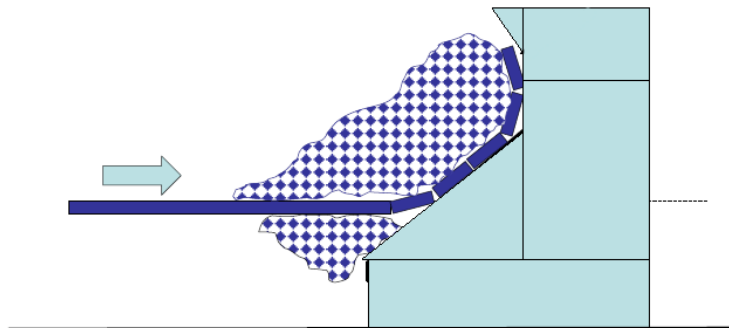
Figure 3.23: Ice Failure on Sloped Structure[17].

The equation proposed in [13]sloping structures,is valid for slopes in the range $0° \leq \alpha < 70°$, where α is the slope measured from a horizontal level.

The horizontal load associated with ice being bent upwards by a cone is:

$$H = A_1[A_2h^2 + A_3\rho_w gh^2 + A_4\rho_w gh^3(D^2 - D_T^2)] \tag{3.22}$$

The vertical downward load is:

$$V = B_1h^2 + B_2\rho_w gh(D^2 - D_T^2) \tag{3.23}$$

where

- $A_1, A_2, A_3, A_4, B_1, B_2$ are dimensionless coefficients which are functions of the ice-to-cone friction coefficient, μ, and the cone angle α. Values of the coefficients are given in the graphs in Figure D.1.

- σ_b is the bending strength of ice, not less than 0.28 σ_c;

- h is the thickness of the ice sheet;

- ρ_w is the density of water;

- g is the gravitational acceleration;

- D is the water line cone diameter;

- D_T is the cone top diameter (often equal to the support structure outer diameter).

For a cone structure that bends ice downwards, the same equations can be used if the water density (ρ_w) is replaced with ice density (ρ_{ice}), and the vertical force direction is reversed to upwards.

These equations are applicable if the cone's height exceeds the ice thickness, either from the top (upward ice action) or from the bottom (downward ice action). The cone's design must ensure that ice crushing occurs only on the cone and not on other parts of the support structure.

The friction coefficient (μ) between ice and cone can be set to 0.15 for concrete or corroded steel cones and 0.10 for new or painted steel cones.

Ice load can be increased due to extra load due to ice rubble buildup on sloping structures. This can be roughly estimated by increasing the ice thickness (h) in the relevant terms of these equations. Additionally, these equations do not consider shear forces from large ice ridges' keel portions.

3.9 Potential Cost Estimation

3.9.1 CAPEX

The Capital Expenditure (CAPEX) for floating offshore wind turbines (FOWT) comprises different catagories such as material costs, fabrication/installation expenses, logistics and transportation, and miscellaneous expenses.Although each categories influences the total investment cost needed for the FOWTs, this study mainly highlighted the cost relating to the impact of ice loads on the cost of the floaters.

The material cost of the floater is estimated as the biggest part of the CAPEX. This involves the cost of secondary steel structure, mooring chains, anchors, connectors, shackles, buoys, floats, and clump weights, etc. The cost of material can be higher due to the higher MBL chain to withstand the ice load. Moreover, to deploy the ice mitigation structure such as ice cones, add up the extra cost for material as well. The details of the cost breakdown is presented in the appendix A.3.

One of the cost components such as Fabrication and installation costs involve labor and equipment expenses, overheads, compliance, and environmental costs. These are crucial since

the installation process might require specialized ice-breaking vessels or additional heating systems to prevent ice formation during the installation process.

Logistic and transportation costs are another important part of the CAPEX since the presence of ice can have major effect in the deployment of the FOWT. The costs associated with sea freight and port fees, which can escalate in icy conditions due to the need for tugboats for towing and icebreaker assistance.

Contingencies cost should be considered in each project for potential unforeseen matters, ensuring financial flexibility and risk management especially In ice-prone areas. The summary of the CAPEX cost breakdown calculation for the FOWTs are shown in the result table 4.12 in section 4.4.1, with detailed information available in the appendix A.3 and highlighted the major cost components which can have high impact in the design consideration, and site selection in terms of financial perspective of the projects. Understanding and managing these cost components is essential to the successful development of the new floating offshore wind windfarm projects, ensuring their economic and operational sustainability.

3.9.2 Operational expenditure (OPEX)for floating platforms

The OPEX includes various cost components which are essential for maintaining the operational efficiency and durability of the wind turbines. The study has been divided into two aspects: which highlighted the ice management measures and the annual operation costs. The total annual operational cost consists of different aspects such as inspection, maintenance, mooring line replacement, and other miscellaneous expenses. Particularly, the most significant individual cost is from the mooring system where the replacement and maintenance which forms a substantial portion of the total OPEX.

Furthermore, the floating offshore wind turbines in ice-prone area incur substantial extra operational costs due to the necessity for ice management measures. This includes costs for ice monitoring systems, icebreaker services and heating systems. The total extra operational cost for ice management is significantly high compared to the standard operational costs, highlighting the significance of effective design consideration and ice management strategies to mitigate these additional costs. The detailed of the OPEX cost breakdown is presented in the table 4.13 in section 4.4.2, with detailed information available in the appendix A.4.

4

Results and Discussion

In this chapter, the findings resulting from the comprehensive design evaluations conducted throughout the thesis will be presented and thoroughly discussed. The results, which are specified in the tables below, will be analyzed to underline the key insights and implications of the study.

4.1 Estimation of Ice loads

4.1.1 Global Horizontal Ice Load

The global ice pressure is determined using equation 3.14, where the empirical coefficients for the size effect, such as m, n, and f_{AR}, are selected based on the width and height of the floater as described in Section 3.5.3. The Global Horizontal Ice Loads for Locations P1, P2, and P3 are then calculated using equation 3.13 and are presented in the table below:

Table 4.1: Estimated Global Horizontal
Ice Load in P1, P2 and P3

Parameter	P1	P2	P3
$h_{50}(\text{m})$	0.255	0.252	0.344
h_c (m)	0.408	0.403	0.550
$C_R(\text{MPa})$	1.331	1.331	1.331
h_1	1	1	1
w	12.5	12.5	12.5
n	-0.449	-0.449	-0.449
m	-0.160	-0.160	-0.160
f_{AR}	0	0	0
$p_G(\text{MPa})$	1.152	1.156	1.057
$F_G(\text{MN})$	5.871	5.824	7.262

The location P3 has the highest ice thickness and hence, has the highest ice pressure and force around 7 MN in magnitude while P1 and P2 yield around 5.8 MN. For floating platforms, the vertical force caused by fluctuating water levels with a fast ice cover adhered to the support structure is not applicable.

4.1.2 Ice Ridge Loads

The overall analysis of all three locations indicates a risk of exposure to ice ridges, as discussed in Section 3.4. Consequently, ice ridge loads are estimated using equation 3.15. One of the primary components of the ridge force is the keel force, which is calculated using equation 3.16, with necessary input parameters detailed in Section 3.5.6.The sail height is computed as 4.2 times the square root of the parent ice thickness (h_p).These inputs are summarized and the ridge loads are estimated in the tables 4.2 and 4.3 below:

Table 4.2: Input Parameters for Ice Ridge Load Calculation

Input Parameter	Value
g (m/s^2)	9.81
ρ_{ice} (kg/m^3)	920
ρ_{water} (kg/m^3)	1007
e, porosity	0.35
ϕ, internal friction angle(deg)	30
c, keel cohesion(KPa)	5000
w(m)	12.5
μ_ϕ	1.732051
γ_e	554.7555

Table 4.3: Ice Ridge Force Calculations

Location	P1	P2	P3
Thk, h_{50} (m)	0.340	0.336	0.458
h_c, consolided (m)	0.544	0.672	0.916
h_p (m)	0.181	0.224	0.305
h_s (m), sail height	1.788	1.988	2.321
h_k,keel height	7.502	8.272	9.529
F_G (MN)	7.129	7.071	8.863
F_k (MN)	2.431	2.779	3.390
F_R (MN)	9.560	9.850	12.253

It was found that keel loads are approximately three times lower than ridge loads. Similar to ice crushing loads, ridge loads also depend on the thickness of the consolidated ice layer. Therefore, Location P3, which has the highest consolidated ice layer, experiences the highest ridge loads, with the keel height reaching around 9.5 meters. In contrast, Locations P1 and

P2 have ridge loads of 9.56 MN and 9.85 MN, respectively, with keel heights ranging from 7.5 to 8.2 meters. The height of the sail is approximately four times less than the keel height.

4.1.3 Ridge Building Load

Based on the equation provided in Section 3.5.7, the ridge building loads are estimated using three ridge generation factors: 2, 6, and 10 because they are the best overall fit to the data collected from embedded sensors and aligns closely with the theoretical value. For R value of 10 intersects the upper bound data points collected for narrower widths (less than 300 meters) and for frozen-in floes but that is not the case for the considered locations. It is a common practice to use a 2 km diameter ice floe size in open Danish waters, including the southern open waters of Denmark. According to ice observations, ice floes of this size or larger have been recorded during ice winters. However, it is important to note that these observation points are located on land and may not accurately represent open water conditions. To adhere to standard Danish practice, the ice floe size is specified as 2 km in diameter [18]. Hence, the pressure (P_D) is calculated using equation 3.20. Based on the literature on ridge building actions, uncertainty factors have been identified in the estimation of ridge building actions from the measured responses. Consequently, a factor of 1.5 is applied to the calculated ice loads to account for these uncertainties [7]. The calculated data are presented below in Table 4.4.

Table 4.4: Ridge Building Load

Location	**P1**			**P2**			**P3**		
h_{50}, (m)	0.255			0.252			0.344		
Ridge generation factor, R	2	6	10	2	6	10	2	6	10
P_D (MN/m)	0.006	0.018	0.030	0.006	0.018	0.029	0.009	0.026	0.043
F_B(MN)	11.9	35.8	59.7	11.8	35.3	58.9	17.4	52.1	86.8
F_B (with load factor) (MN)	17.9	53.8	89.6	17.6	53	88.4	26	78.1	130.2

The ridge building loads, calculated with an R factor of 2, result in the lowest ice loads across all three locations, while an R factor of 10 produces the highest loads. When applying the uncertainty factor of 1.5, the ridge generation loads range from 17 MN to 89 MN for Locations P1 and P2. For Location P3, the loads vary from 26 MN to 130 MN. This variation indicates that Location P3 experiences a wider range of potential ice loads compared to P1 and P2, reflecting its higher ice consolidation layer and resulting in greater susceptibility to ridge loads.

4.1.4 Blockage Effect

The blockage effect is more pronounced with first-year ice ridges (FY ridges), where ice rubble in the keel can significantly restricted the motion between the legs. Without blockage, the individual leg loads at Points 1, 2, and 3 consider factors like the global leg crushing load and keel load. However, when the effective blocked width is considered, the loads significantly increase. The estimated data are presented in below table 4.5.

Table 4.5: Multi Leg Ice Jamming Evaluation

Point 1								
Leg Spacing (m)	No. of Legs	Leg Factor	Blocked Width (m)	Leg Crushing Load (MN)	Leg Keel Load (MN)	Leg Rubbling Load (MN)	Leg Total Load (MN)	Global Leg Load (MN)
40.5	4	0.7	0	5.5	7.9	17.9	31.3	89.0
40.5	4	0.7	90.1	18.5	58.6	17.9	95.0	269.8
Point 2								
Leg Spacing (m)	No. of Legs	Leg Factor	Blocked Width (m)	Leg Crushing Load (MN)	Leg Keel Load (MN)	Leg Rubbling Load (MN)	Leg Total Load (MN)	Global Leg Load (MN)
40.5	4	0.7	0	5.5	8.2	17.7	31.3	88.9
40.5	4	0.7	90.1	39.4	82.2	17.7	139.3	395.6
Point 3								
Leg Spacing (m)	No. of Legs	Leg Factor	Blocked Width (m)	Leg Crushing Load (MN)	Leg Keel Load (MN)	Leg Rubbling Load (MN)	Leg Total Load (MN)	Global Leg Load (MN)
40.5	4	0.7	0	6.6	9.8	26.0	42.4	120.5
40.5	4	0.7	90.1	47.8	94.4	26.0	168.3	477.8

[a] MN = Mega Newton

Since, the gap distance by width (L/w) ratio is less than 5 for the reference floater, the risk of ice blockage effect needs to be considered. To mitigate the risk of ice jamming, several design strategies can be implemented. These include increasing the spacing between the legs to achieve a higher L/w ratio, thereby reducing the likelihood of ice accumulation. Additionally, incorporating design features that minimize ice interaction, such as sloped surfaces or ice-

breaking structures, can help manage ice loads more effectively.

4.2 Results from Orcaflex

The tension in mooring lines 2 and 3 are identical due to the symmetrical shape of the floater for all three design points. However, due to the ice load, wave, current and wind uni-direction for conservative scenario, Mooring line 1 consistently encounters the highest tension across all Design Load Cases (DLCs). DLCs 1.6 and 6.1 represent scenarios with no ice load, while DLCs 9.1 to 9.5 correspond to different ice events, as detailed in Section 3.7.1 and Table 3.6. For all design location point P1,P2 and P3, the effective tensions in all mooring lines are provided in Tables 4.6, 4.7, and 4.8 respectively.

As shown in the table below, the highest ice load scenarios can be seen in DLCs 9.1 and 9.5, which consider a 50-year return period ice thickness. Thus, the tension in mooring lines during these load cases is significantly higher than in other DLCs. Particularly, the effective tension in Mooring line 1 reaches a maximum of 19.5 MN at location P3, which is higher than at the other two locations due to the increased ice loads.

According to the API standard [16], the maximum allowable tension in a mooring line should not exceed 60% of the mooring chain's Minimum Breaking Load (MBL) in the dynamic analysis of Intact condition. To withstand the ice loads and maintain the station while experiencing these scenarios, it is required to upgrade the mooring system. Consequently, mooring chains with higher MBLs are recommended, as indicated in Table 4.9.

Table 4.6: Effective Tension for Various Design Load Cases (DLCs)For Point 1 in MegaNewtons (MN)

DLC	Applied Ice Load (MN)	Effective Tension (MN)		
		Mooring1	Mooring2	Mooring3
1.6	0.00	5.93	2.10	2.10
6.1	0.00	4.30	2.42	2.42
9.1	11.89	16.72	1.69	1.69
9.2	6.87	11.71	1.73	1.73
9.3	10.67	13.32	1.76	1.76
9.4	6.87	9.48	1.82	1.82
9.5	11.89	14.53	1.75	1.75

Table 4.7: Effective Tension for Various Design Load Cases (DLCs)For Point 2 in MegaNewtons (MN)

DLC	Applied Ice Load (MN)	Effective Tension (MN)		
		Mooring1	Mooring2	Mooring3
1.6	0.00	7.35	2.08	2.08
6.1	0.00	6.58	2.37	2.37
9.1	11.79	16.61	1.69	1.69
9.2	6.72	11.55	1.73	1.73
9.3	10.99	13.63	1.76	1.76
9.4	6.72	9.33	1.82	1.82
9.5	11.79	14.43	1.76	1.76

Table 4.8: Effective Tension for Various Design Load Cases (DLCs)For Point 3 in MegaNewtons (MN)

DLC	Applied Ice Load (MN)	Effective Tension (MN)		
		Mooring1	Mooring2	Mooring3
1.6	0.00	6.80	2.08	2.08
6.1	0.00	5.07	2.38	2.38
9.1	14.71	19.47	1.68	1.68
9.2	7.34	12.09	1.72	1.72
9.3	13.61	16.16	1.75	1.75
9.4	7.34	9.86	1.81	1.81
9.5	14.71	17.26	1.74	1.74

Table 4.9: Suggested Mooring Design due to the Ice Loads

Location	Chain Type	Chain(mm)	Breaking Load (MN)	60% of MBL	Maximum Effective Tension	Status
P1	R4 studless chain	188	28.05	16.83	16.72	**Pass**
P2	R4 studless chain	187	27.83	16.7	16.61	**Pass**
P3	R4 studless chain	209	32.65	19.59	19.47	**Pass**

4.3 Ice Mitigation Measures(Ice Cone)

Ice cones have been widely adopted as a cost-effective and highly efficient ice mitigation strategy over the past few decades. Consequently, the application of ice cones for floating structures is recommended. The ice loads on these sloped structures are estimated using equations 3.22 and 3.23. The necessary inputs, including the dimensionless coefficients, are detailed in Appendix A.2, while additional inputs are specified in Section 3.8.1. The resulting data are presented in the table below:

Table 4.10: Ice Load estimation for vertical structure with (ice Cone)Sloping Structure

Parameter	Value
μ, ice to cone friction	0.1
α (deg)	45
D (m)	18.5
D_T (m)	12.5
g (m/s^2)	9.810
ρ_w kg/m^3	1007.000
h (m)	0.344
σ_f (Pa)	500000
A_1	2.7
A_2	0.04
A_3	0.325
A_4	1.3
B_1	1.08
B_2	0.04
Horizontal load, ride up	**1.069 MN**
Vertical load, downward	**0.051 MN**

The implementation of ice cones significantly reduces the ice loads on the structure. The results indicate a substantial decrease in both horizontal and vertical loads when ice cones are used. Specifically, the horizontal crushing load without the ice cone is 7.26 MN. With the use of ice cones, the horizontal ride-up load is reduced to 1.07 MN, and the vertical downward load is 0.05 MN. This reduction translates to an approximate 85% decrease in the horizontal load. Such significant reductions demonstrate the effectiveness of ice cones in mitigating ice loads, thereby enhancing the structural integrity and reducing the potential for ice-induced damage.

Table 4.11: Comparison of Ice Loads With and Without Ice Cones

Load Description	Magnitude (MN)
Horizontal Crushing Load, F_G (without ice cone)	7.26
Horizontal Load Ride-Up (with ice cone)	1.07
Vertical Load Downward (with ice cone)	0.05

4.4 Cost Comparison

4.4.1 CAPEX

The CAPEX breakdown is summarized in the table below and a few highlights of the cost are presented. Material Cost dominates the total CAPEX at 80%, followed by Contingencies at 9%, and Fabrication Installation Cost at 10%. The remaining costs are Logistic, Transportation and other Expenses which contribute only a small portion of the total CAPEX. The CAPEX of the floater is extimated to be approximately 5.3 million euros.

Table 4.12: CAPEX Breakdown

Expense Category	Amount(€)
Material Cost	4,222,357
Fabrication Installation Cost	548,071
Logistic and transportation	28,399
Other Expenses (permit and Inspection)	7,000
Contingencies (10% of CAPEX)	480,583
Total CAPEX	**5,286,410.34**

4.4.2 OPEX

Annual OPEX estimation includes various cost components such as inspection, maintenance, and insurances, etc. Among these, mooring line replacement has the highest percentage around 58% of the total OPEX cost. Operational Management and contingency fund account for 10% each of the total, while the remaining components made up to a small fraction of the total OPEX cost, which is around 220,000 euro annually. The detail breakdown of the OPEX can be seen in the table 4.13 below:

Table 4.13: Annual Operation Cost

Operational Cost Estimates	
Cost Component	Annual Cost (€)
Inspection Costs	€ 15,000
Maintenance Costs	€ 10,000
Mooring Line Replacement	€ 127,500
Buoy/Float Replacement	€ 960
Connector/Shackle Replacement	€ 3,000
Operational Management	€ 20,000
Monitoring Equipment	€ 5,000
Insurance Costs	€ 10,000
Regulatory Compliance	€ 5,000
Miscellaneous Expenses	€ 3,000
Contingency Fund (10%)	€ 19,946
Total Annual Operational Cost	€ 219,406

4.4.3 Comparison of the CAPEX and OPEX in P1, P2 and P3 with IM measures

In this section, the CAPEX of the FOWTs in P1, P2 and P3 are analysed. Material costs across the three locations are the most significant expense, accounting for 80% of the total cost. Since, the suggest mooring chains in P1 and P2 have similar weights per meter, subsequently, the costs for both locations are approximately the same while P3 has bigger chain to withstand the ice loads, the material cost for P3 shows significant increase. The material cost of the ice cones for all four legs of the floater has been included in the estimation. Additionally, a mandatory contingencies fund is estimated at 10% of the total cost.The detailed breakdown and comparison are presented in the below table 4.14.

Table 4.14: CAPEX Estimation for Ice Mitigation Measures

CAPEX Estimation for Ice Mitigation Measures			
Expense Category(€)	**P1**	**P2**	**P3**
Material Cost	6511160	5460922	5509209
Fabrication/Installation Cost	811283	690506	696059
Logistic and transportation	28399	28399	28399
Other Expenses (permit and Inspection)	7000	7000	7000
Contingencies (10% of CAPEX)	735784	618683	624067
Total CAPEX	**8093627**	**6805510**	**6864734**

The OPEX estimation for ice management measures are crucial in cost estimation of the whole project. A significant component of the IM measures is the using of semi-passive IM strategies which involves deployment of tugboats and ice breaker vessels. The operation costs were estimated based on the number of freezing degree days and it accounts for the big portion of the total cost approximately 90%. The ice management costs for all thress loactions are summarized in the table 4.15.

Table 4.15: OPEX Estimation for Ice Mitigation Measures

Ice Management Costs			
Cost Component	**Annual Cost (€)**		
Ice Monitoring Systems	10000	10000	10000
Icebreaker Services	1292000	1224000	1530000
Heating Systems	2000	2000	2000
Fuel and Energy Costs	3800	3600	4500
Ice-Related Repairs	10000	10000	10000
Contingency	129780	122960	153650
Total Extra Operational Cost	1447580	1372560	1710150

The total CAPEX and OPEX both with and without the Ice Management measures are summarized in the table below 4.16.

Table 4.16: Summary of Cost comparison

Cost Category (€)	Location		
	P1	**P2**	**P3**
CAPEX without IM measures	5286410	5286410	5286410
CAPEX with IM measures(Ice Cone and Chain)	6864734	6805510	8093627
OPEX (Annual)	219406	219406	219406
OPEX(IM)	1447580	1372560	1710150

This page intentionally left blank.

5

Conclusion and Furthur Scope

5.1 Conclusion

In this section, the key points and findings of the study are summarized, providing a comprehensive overview of the design methodologies and the insights gained. The study has systematically researched about the feasibility of deploying floating offshore wind turbines (FOWTs) in ice-infested waters within the Baltic Sea in various aspects. The thesis distinguishes the ice conditions on the selected area and impact of different ice loads on both the structural and the mooring systems of FOWTs. Additionally, the suggestion of the implementation of robust ice management strategies and potential cost estimation to deploy the whole concept ensuring operational safety and feasibility.

Key findings include the environmental conditions and ice type formation in the region where very severe winters occurred in the 1940s and severity has been reduced in recent years due to the global warming. As suggested, the location P3 experiences the longest winter with the higher frost index than the location P1 and P2 for the 50-year return period. Consequently, the ice thicknesses derived from the frost index also show thicker in the P3 around 34 cm and 25 cm in P1 and P2. Based on the 50-year return ice thicknesses, various ice loads are estimated mainly, global ice crushing load, ice ridge loads and ridge building loads. The global ice crushing loads are varying from 5.8 to 7.3 MN. Ridge forces are ranging from 7.9 to 10 MN while the keel loads are resulting from 2 to 2.8 MN. Ridge building loads are evaluated using the ridge building load factor 2,6, and 10 and the lowest factor gives the lowest ridge building load around 17 MN in P1 and P2 and 26 MN in P3. Another concerning ice event, ice blockage or ice jamming, is evaluated and discussed in this thesis, where L/w ration plays a significant part in this matter. The floater has the L/w lower than 5 and hence, higher risk to expose to the ice blockage effect. The loads of the individual legs are estimated. By following the standard regulations, ice loads are simulated with various DLCs integrating the different environmental conditions and ice events, including the environmental load factor and dynamics magnification factor . Due to the increased ice loads, there is a significant effect in the mooring system of the floater. The effective tensions in the mooring lines are found insufficient to maintain since it has lower strength than the 60% of the MBL. To maintain the structural integrity and position of the floater, mooring system must be upgraded with higher strength chains. Following by the different ice loads and events, ice mitigations systems are considered to manage the floater in the selected regions. Using constructive ice measures, such as ice cones are the most effective and cost -efficient IM strategies, as the ice loads on the sloped surface are significantly lower than the vertical structures. Moreover, using IM equipment and system can deliver effective outcomes but the initial cost of the project has increased due to those extra IM measures. Consequently, the potential costs CAPEX and

OPEX are estimated considering all the extra expenditure due to the IM strategies. Mainly, the material cost accounts for most of the total cost. The increase in CAPEX for P1 and P2 is around 30% of the initial CAPEX and since P3 need higher strength chain due to higher ice loads, the cost is higher with approximately 50% increase. Overall, this thesis contributes significantly to the understanding of the impact of deploying floating platforms in the ice prone regions. The results presented here serve as a foundation for future developments into colder and more challenging regions and safe expansion of offshore wind energy and achieve the energy goal in Europe.

5.2 Future Scopes

Effect of Dynamic Ice Load on Floater Response:

The dynamic effect of ice loads, particularly those resulting from interactions of ice floes and ridges with the structure, has a profound impact on the structural response of FOWTs. Future studies should focus on a more detailed analysis of ice induced vibrations on the floating platforms and exploration of fatigue life of structure due to those vibratory loads.

Response of Different Floating Foundations to Ice Loads:

While this thesis focused only on semi-submersible floating foundation, the response of other floater designs to ice loads in the Baltic region is an interesting perspective to explore. Future research could involve studying various types of floating platforms, such as spar buoys or tension leg platforms, to comprehend how different designs impact on the floater's performance due to ice loads.

Exploration of Alternative Mooring Configurations:

The reference mooring line configuration in this thesis utilized single catenary mooring arrangement. To further optimize the design of FOWTs in ice-infested waters, future work should research the impacts of mooring system with different configurations and compositions. This could involve analyzing the performance of mooring lines made from various materials composition, as well as different configurations, such as taut versus slack mooring systems and using polyester cables.

Comparative Analysis of Ice Management (IM) Strategies:

IM measures discussed in this thesis covers different systems such as active and passive IM systems, but a comparative analysis of these strategies using different models and ice events would be interesting to explore. Future research could include a comparison of existing IM strategies with the model used in this study, to identify the most effective solutions for ice mitigation.

Bibliography

[1] Global Wind Energy Council (GWEC). (2023). *Global Wind Report 2023*. Retrieved from https://gwec.net/global-wind-report-2023/

[2] World Wind Energy Association (WWEA). *World Wind Energy Report 2023*. Retrieved from https://wwindea.org/blog/2023/06/12/world-wind-energy-report-2023/

[3] Costanzo, G., Brindley, G. (2024). *Wind Energy in Europe - 2023 Statistics and the Outlook for 2024-2030*. WindEurope. Additional contributors: Willems, G., Ramirez, L., Cole, P., Klonari, V. Editor: O'Sullivan, R. Design: Van de Velde, L. Photo cover: Bickley, J.

[4] European Commission. (2021). *The European Green Deal*. Retrieved from https://ec.europa.eu/info/strategy/priorities-2019-2024/european-green-deal_en

[5] Lee, C. H. (1995). WAMIT User Manual. Massachusetts Institute of Technology.

[6] Hall, M. and Goupee, A. (2015). MoorDyn User Guide. University of Maine.

[7] International Organization for Standardization (ISO). (2019). *ISO 19906:2019 Petroleum and natural gas industries – Arctic offshore structures*. Retrieved from https://www.iso.org/standard/64790.html

[8] DNV GL. (2019). *DNV-ST-0437: Loads and site conditions for wind turbines*. Retrieved from https://rules.dnv.com/docs/pdf/DNV/ST/2019-12/DNV-ST-0437.pdf

[9] DNV GL. "DNVGL-RP-C205: Environmental Conditions and Environmental Loads." 2015.

[10] Det Norske Veritas AS. (2013). *DNV-OS-J103: Design of Floating Wind Turbine Structures*. Offshore Standard, June 2013. Available at: http://www.dnv.com

[11] Det Norske Veritas AS. (2014). *DNV-OS-J101: Design of Offshore Wind Turbine Structures*. Offshore Standard, May 2014. Available at: http://www.dnv.com

[12] Offshore Installations, IV Part 6, Chapter 7, Oil and Gas, Guidelines for the Construction of Fixed Offshore Installations in Ice Infested Waters, Germanisher Lloyd. GL Edition 2005.

[13] International Electrotechnical Commission (IEC). (2019). *IEC 61400-3-1: Design requirements for offshore wind turbines*. Retrieved from https://webstore.iec.ch/publication/64778

[14] International Electrotechnical Commission (IEC). (2019). *IEC 61400-3-2: Design requirements for floating offshore wind turbines*. Retrieved from https://webstore.iec.ch/publication/64779

[15] American Bureau of Shipping (ABS), *Guide for Building and Classing Floating Offshore Wind Turbine Installations*, 2020.

[16] API. (2005). *API Bulletin 2SK Addendum 2: Design and Analysis of Stationkeeping*

Systems for Floating Structures. Retrieved from `https://www.api.org/~/media/files/news/hurricane/2sk_add.pdf`

[17] Croasdale, K. R. (2012). *Arctic Offshore Engineering*. Retrieved from `https://www.researchgate.net/publication/312378862_Arctic_Offshore_Engineering`

[18] Jørgensen, L. B., Bäckström-Andreasen, S., Olrik, A. (2024). *Ice Assessment, Energy Island Baltic Sea Bornholm I and II OWF*. Sweco. Project Number: 41007612. Document Number: 41007612-001. Client: Energinet. Version 03, 16 February 2024.

[19] Lars Bülow Jørgensen, Sabine Bäckström-Andreasen, and August Olrik. *Ice Assessment SKF Ver. 4 240104*. Sweco, 2024. Controlled by Helge Gravesen.

[20] Helge Gravesen and Tuomo Kärnä. *Ice Loads for Offshore Wind Turbines in Southern Kattegat*. In: Proceedings of the 20th International Conference on Port and Ocean Engineering under Arctic Conditions (POAC 09), June 2009.

[21] Hayo, M. (2020). *Ice Measures for Offshore Wind Farms*. Retrieved from `https://www.researchgate.net/publication/342347987_Ice_Measures_for_Offshore_Wind_Farms`

[22] Port of Gothenburg, *The Largest Port in Scandinavia*, `https://www.portofgothenburg.com/`, [Accessed 22-07-2024].

[23] Bornholm Energy Island, *Denmark's Hub for Renewable Energy*, `https://stateofgreen.com/en/partners/energy-island-bornholm/`, [Accessed 22-07-2024].

[24] Stockholm University, *Ice Conditions in the Baltic Sea*, `https://www.su.se/english/research/research-areas/climate-seas-and-environment`, [Accessed 22-07-2024].

[25] Hetmanczyk, S., Heinonen, J., Strobel, M. (2011). *Dynamic ice load model in overall simulation of offshore wind turbines*. In Proceedings of the 21st International Offshore and Polar Engineering Conference (ISOPE).

[26] Liu, Z. (2022). *Offshore Structure Design Under Ice Loads*. In Encyclopedia of Ocean Engineering. Springer, Singapore. doi:10.1007/978-981-16-6924-7.

[27] Ji, S., Di, S., Liu, S. (2015). *Analysis of ice load on conical structure with discrete element method*. Engineering Computations, 32(1), 217-236. doi:10.1108/EC-03-2013-0071.

[28] Høyland, K. V., et al. (2023). *Challenges with sea ice action on structures for Offshore wind*. Proceedings of the 27th International Conference on Port and Ocean Engineering under Arctic Conditions (POAC), Glasgow, United Kingdom.

[29] Høyland, K. V., et al. (2023). "Comprehensive Study on Ice-Structure Interactions in the Baltic Sea." *Journal of Cold Regions Engineering*.

[30] Orcina Ltd, "Environment," Available: `https://www.orcina.com/webhelp/OrcaFlex/Content/html/Environment.htm`.

[31] Orcina Ltd, `https://www.orcina.com/orcaflex/`.

[32] Subodh Kumar, Babloo Chaudhary, Manu K. Sajan, P. K. Akarsh, "Response of Offshore Wind Turbine Foundation Subjected to Earthquakes, Sea Waves and Wind Waves: Numerical Simulations," *SpringerLink*, Available: `https://link.springer.com/article/10.1007/sXXXXX-XXX-XXXX-XX`.

[33] Marina Dock Age, "Winterization and Ice Mitigation Strategies," available at: `https://www.marinadockage.com`, accessed July 2024.

[34] NRDC, "New Recommendations Reduce Floating Wind Entanglement Risk," available at: `https://www.nrdc.org`, accessed July 2024.

[35] Offshore Renewable Energy Catapult, *Mooring and Anchoring BOMs and Summary Report*, 2023, Draft 1.

[36] National Renewable Energy Laboratory (NREL), *Offshore Wind Cost Reduction Pathways Study*, 2021.

[37] Definition of the UMaine VolturnUS-S Reference Platform , `https://www.nrel.gov/docs/fy20osti/76773.pdf`.

[38] International Energy Agency (IEA), *World Energy Investment 2022*, 2022.

This page intentionally left blank.

A

Appendix

A.1 Metocean Data from DHI

A.1.1 Wave Data
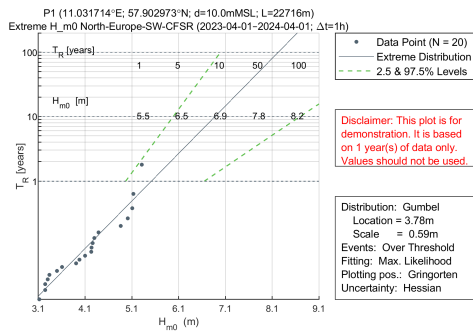
Figure A.1: P1 Extreme H$_{m0}$
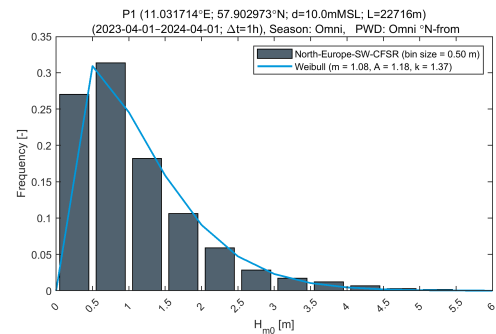
Figure A.2: P1 Weibull Fit H$_{m0}$
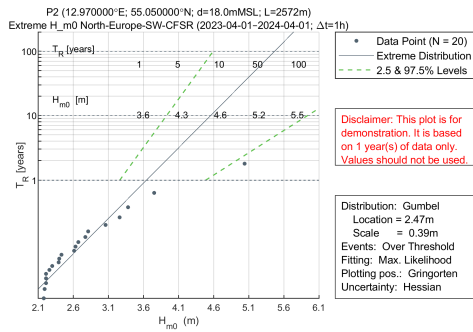
Figure A.3: P2 Extreme H$_{m0}$
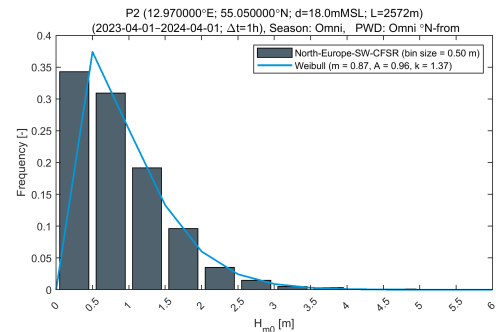
Figure A.4: P2 Weibull Fit H$_{m0}$
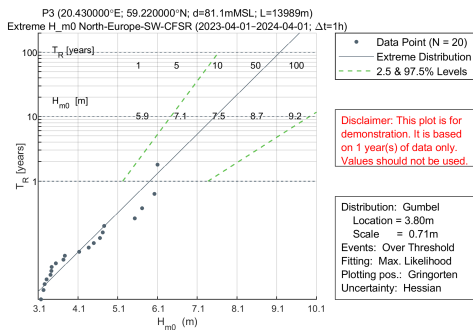
Figure A.5: P3 Extreme H$_{m0}$
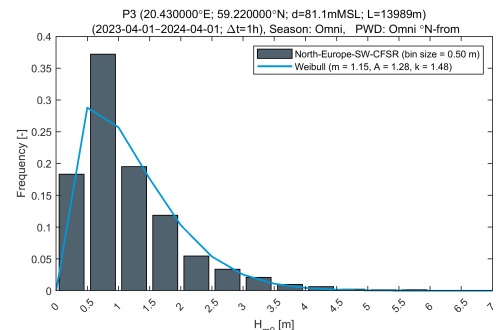
Figure A.6: P3 Weibull Fit H$_{m0}$

A.1.2 Current Data
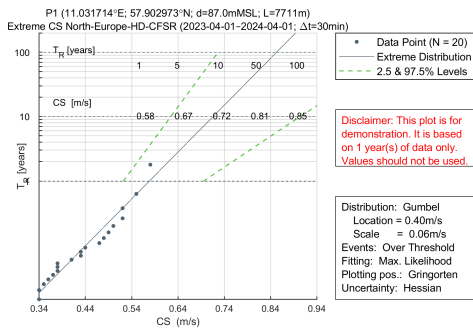
Figure A.7: P1 Extreme CS
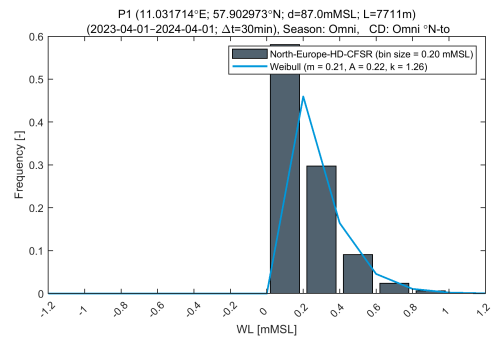
Figure A.8: P1 Weibull Fit WL
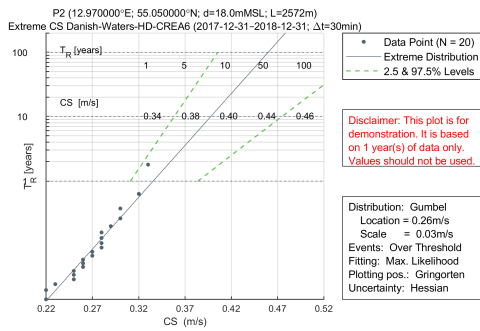
Figure A.9: P2 Extreme CS
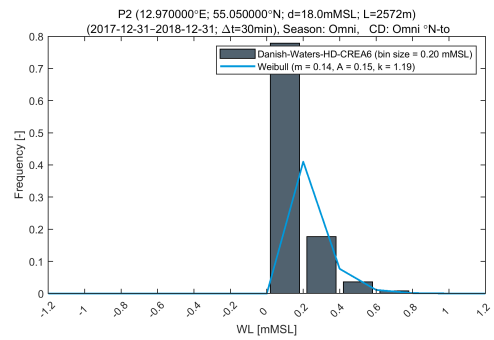
Figure A.10: P2 Weibull Fit WL
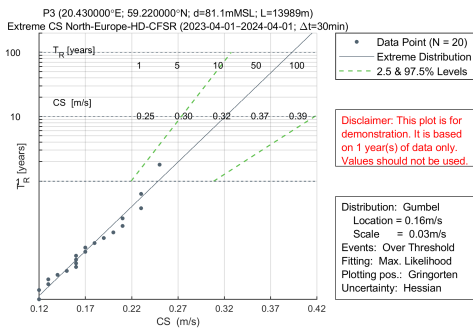
Figure A.11: P3 Extreme CS
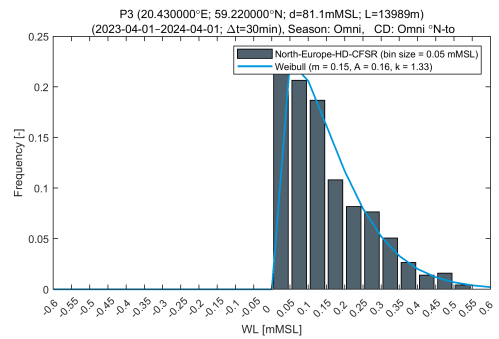
Figure A.12: P3 Weibull Fit WL
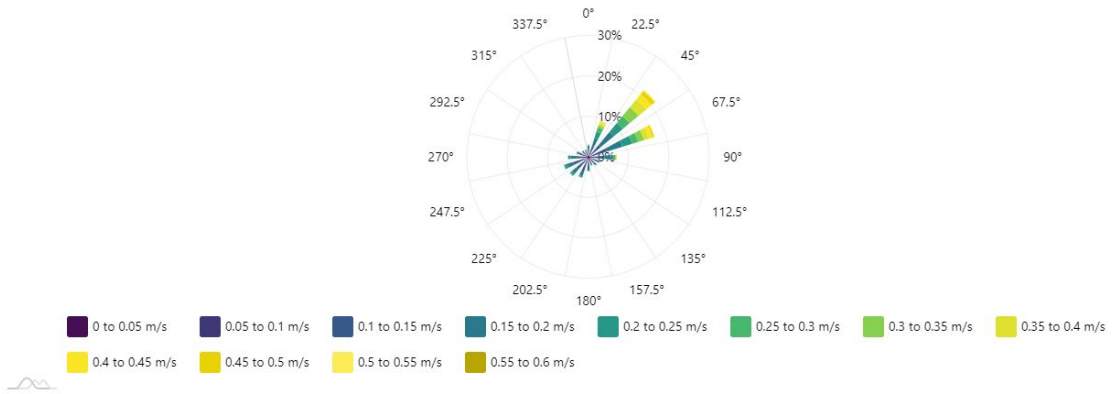
(a) P1 Current Speed Rose Plot
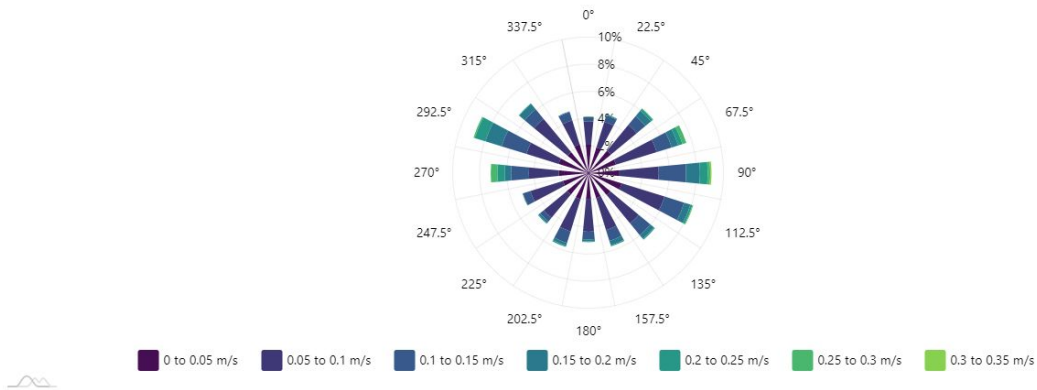
(b) P2 Current Speed Rose Plot
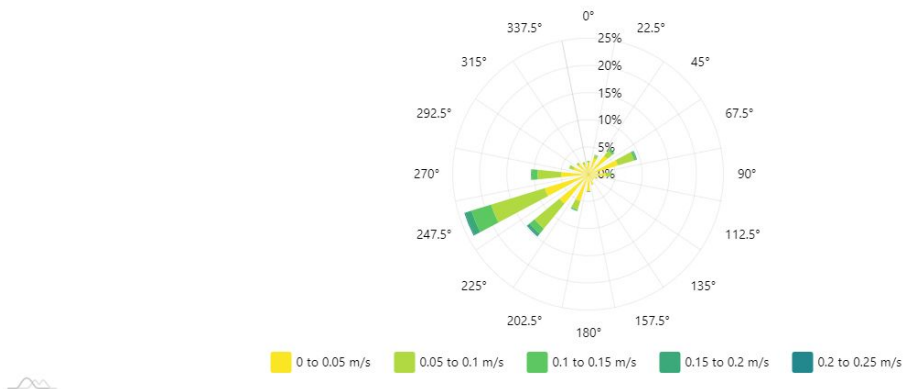
(c) P3 Current Speed Rose Plot

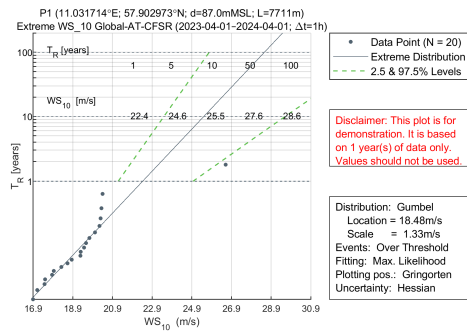**Figure A.13:** Current Speed Rose Plots for Different Points
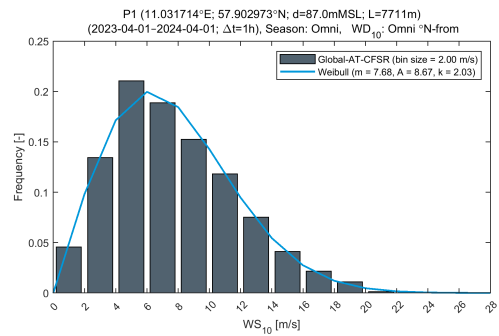
A.1.3 Wind Data

Figure A.14: P1 Extreme WS10

Figure A.15: P1 Weibull Fit WS10
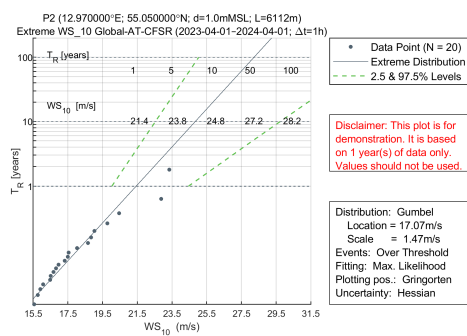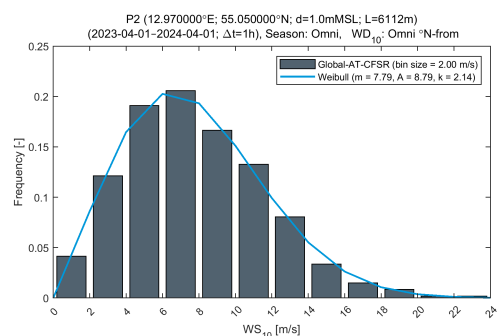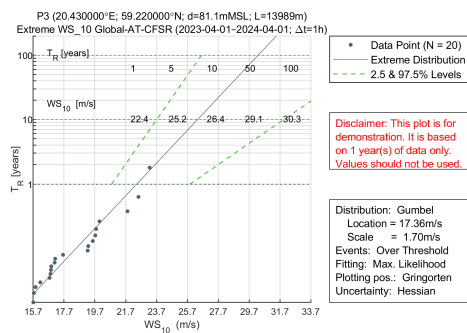

Figure A.16: P2 Extreme WS10

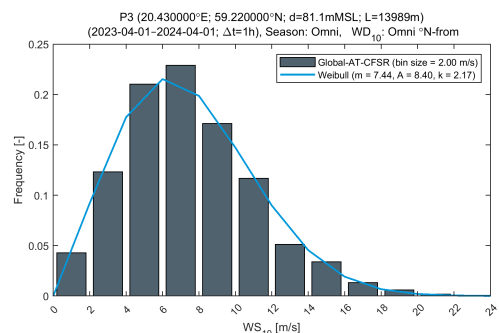**Figure A.17:** P2 Weibull Fit WS10

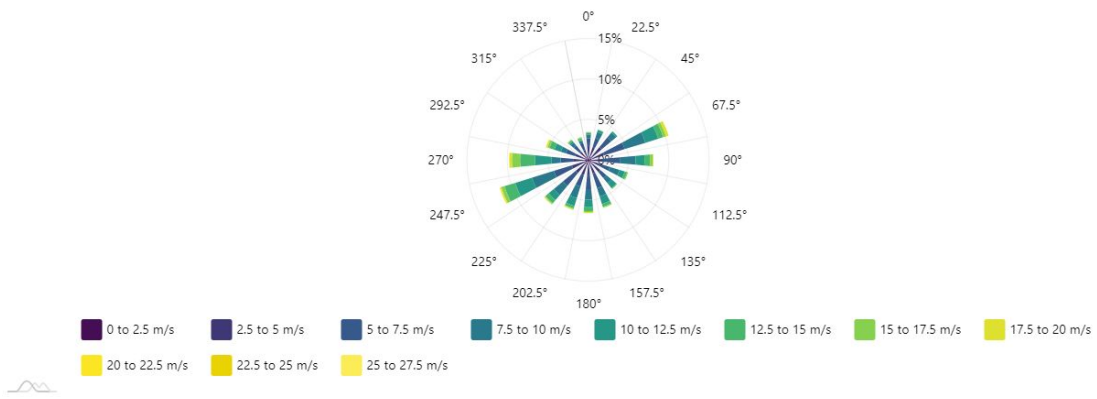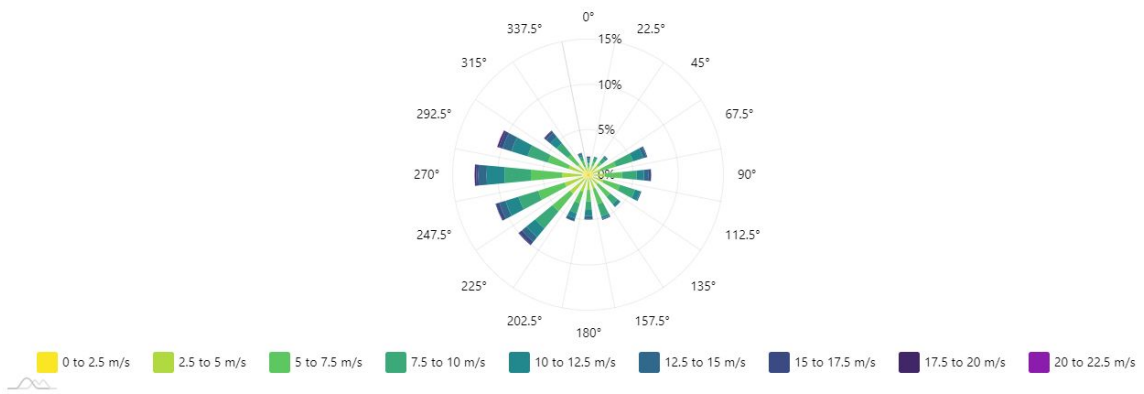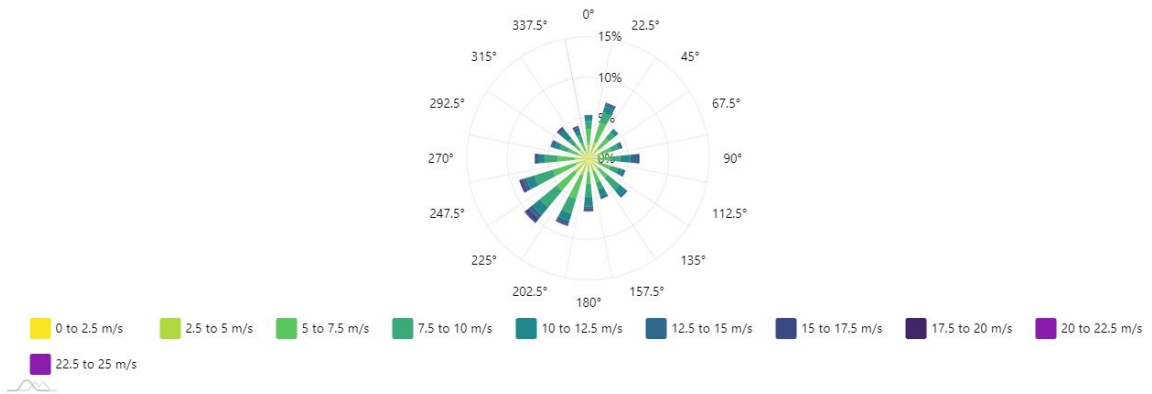**Figure A.18:** P3 Extreme WS10

Figure A.19: P3 Weibull Fit WS10
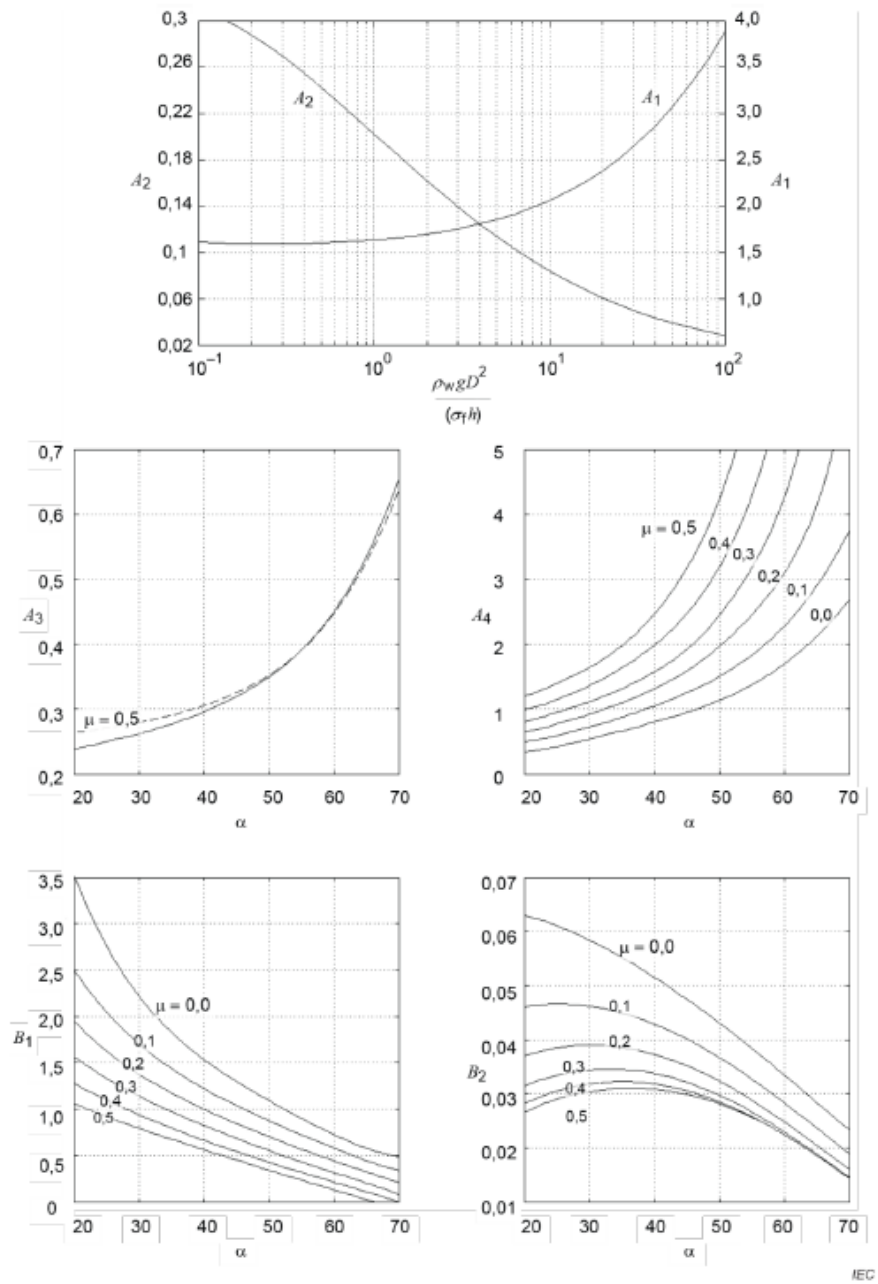
(a) P1 Wind Speed Rose Plot

(b) P2 Wind Speed Rose Plot

(c) P3 Wind Speed Rose Plot

Figure A.20: Wind Speed Rose Plots for Different Points

A.2 Ice Load

Figure A.21: Ice Load Coefficient for slope structure[13].

A.3 Potential Cost

Table A.1: Detailed CAPEX Estimation (Material Cost) of the mooring system without using Ice cones and Ice loads

MATERIAL COST(without ice cone)		
R3 Studless Mooring Chain 185 dia:		
Length of mooring line	850	m
No of mooring line	3	
weight	685	kg/m
cost of chain	2367	euro/tonne
total weight	1747	tonne
sub-Total	4134557	€
Anchors		
No. of anchor	3	
cost/unit	20000	€
sub-Total	60000	€
Connector and Shackles		
No. of unit	30	(10 per each line)
cost/unit	300	€
sub-Total	9000	€
Bouys and Floats		
No. of unit	6	(2 per each line)
cost/unit	800	€
sub-Total	4800	€
Clump Weights:		
No. of unit	6	(2 per each line)
cost/unit	1500	€
sub-Total	9000	€
Anti-chafing Gear:		
Estimated Cost	5000	€
Total Material Cost	4222357	€

Table A.2: Detailed CAPEX Estimation(Fabrication Cost) of the mooring system without using Ice cones and Ice loads

FABRICATION/INSTALLATION COST		
Labour Cost		
Working Hr	1000	hr
Labour Rate	50	€/hr
sub-Total	50000	€
Equipment Cost		
cold/hot Work (10% of Material Cost)	422236	€
sub-Total	422236	€
Direct Cost	472236	€
Overhead and Misc		
15% of Direct Cost	70835	€
Compliance and Environment Cost		
Estimated Cost	5000	€
Total	548071	€

Table A.3: Detailed CAPEX Estimation(Logistic and transportation) of the mooring system without using Ice cones and Ice loads

Logistic and transportation		
Material Handling Cost		
Loading/unloading	2000	(10 per each line)
Storage	1000	€
Shipping		
Sea freight (10 € per 1000 kg)	17818	€
Port Fees	1500	€
On site logistics		
Installation and transport	3500	€
Contingency	2582	€
Total	28399	€

Table A.4: Annual Operation Cost

Operational Cost Estimates	
Cost Component	Annual Cost (€)
Inspection Costs	€ 15,000
Maintenance Costs	€ 10,000
Mooring Line Replacement	€ 127,500
Buoy/Float Replacement	€ 960
Connector/Shackle Replacement	€ 3,000
Operational Management	€ 20,000
Monitoring Equipment	€ 5,000
Insurance Costs	€ 10,000
Regulatory Compliance	€ 5,000
Miscellaneous Expenses	€ 3,000
Contingency Fund (10%)	€ 19,946
Total Annual Operational Cost	€ 219,406

A.4 Lists

Listing A.1: Metocean data anlysis

```python
import pandas as pd

# Path Definition
file_path = 'D://Nann Thesis//P1_Global_AT_CFSR_11.031714_57
    .902973_10_22716.1_1979-01-01_2024-04-01_.csv'

# Load the data from the CSV file.
data = pd.read_csv(file_path, header=14, parse_dates=[0])

# First column rename
data.columns = ['Date'] + list(data.columns[1:])

# Skipping row 14
temperature_data = data.iloc[15:].copy()

# Convert 'Date' column to datetime
temperature_data['Date'] = pd.to_datetime(temperature_data['
    Date'])

# Set the 'Date' column as the index for resampling
temperature_data.set_index('Date', inplace=True)

# Data Resampling
daily_averages = temperature_data.resample('D').mean()

# Filter to have days with specific temperature range
cold_days = daily_averages[daily_averages["Air Temperature
    at 2m (T_{air}) [\Deg.C]"] < -0.4].copy()

# Year Extraction
cold_days['Year'] = cold_days.index.year


cold_days_per_year = cold_days.groupby('Year').size().
    reset_index(name='Number of Cold Days')

# Excel file path
output_file_path = 'D://Nann Thesis//
    Cold_Daily_Temperature_AveragesP1---.xlsx'
```

```
36
37      # Writing Excel File
38      with pd.ExcelWriter(output_file_path, engine='openpyxl') as
            writer:
39          # Write the averages
40          cold_days.to_excel(writer, sheet_name='Cold Daily
                Averages', index_label='Date')
41
42          # Write the count of cold days per year to another sheet
43          cold_days_per_year.to_excel(writer, sheet_name='Cold
                Days Per Year', index=False)
44
45          # Write the overall daily averages to another sheet
46          daily_averages.to_excel(writer, sheet_name='Daily
                Averages', index_label='Date')
47
48
49      print(f"Cold daily averages, yearly counts, and daily
            averages successfully written to {output_file_path}")
```